List of Figures

List of Tables

Chapter 1

Introduction

1.1 General Background

Materials have been the milestone of progress of humankind. All civilizations have been categorized by the materials they used; the stone age, the bronze age, the steel age etc. Some of these periods in history lasted centuries but in recent times both the rate of major materials breakthroughs and their improvements are happening rapidly. During the 20^{th} century, virtually every aspect of the human life, from clothing to construction, changed profoundly by new materials. High performance materials made possible some of the century's most dazzling technological achievements: airplanes and spacecraft, microchips and magnetic disks, lasers and the fiber-optic highways. Behind all these are the ability of scientists and engineers to customize the materials for particular applications by manipulating its composition and microstructure: they start with a requirement. These are three major classes of materials metals, polymers and ceramics. The combination of two or more of these materials together to produce a new material whose properties would not be attainable by conventional means is called a composite. In the last half century, the growth of materials technology has been explosive, and its impact on our daily lives pervasive. The use of plastics is now so widespread that it is difficult to imagine life without them. Today, metals unknown in ancient times, such as aluminium and titanium, play a leading role in modern technology. These metals are widely used, for instance, in the aircraft industry because of their low densities and high resistance to corrosion. The ceramics which were the first engineering materials, finding application as building materials and pottery in the stone age, recent technological advances combined with their unique electrical properties, hardness, durability and heat resistance are making ceramics the material of the future.

Beginning with the invention of the transistor in 1950's, the electronics revolution, enabled by advances in materials has dramatically and irreversibly changed our lives. The electrical industry and its flourishing daughter the electronics industry, uses a great variety of dielectric and insulation materials and they have constantly evolved over the years by the development of new and better materials. Ni-Zn and Mn-Zn ferrites found increasingly widespread use as transformer and coil core materials in telephones and in radio receivers in early 1920's. Some other electro-ceramics exhibit optical phenomena, such as luminescence (useful in fluorescent lighting) and lasing (exploited in lasers) and still others exhibit changes in optical properties with the application of electric fields and are therefore used extensively as modulators, demodulators and switches in optical communications. Perhaps, nowhere has the promise of ceramics been more tantalizing than in the quest for materials called superconductors, which can carry electric current with zero resistance. The applications of these materials have even spread into the medical field. Surgeons are already using bio-ceramic materials for repair and replacement of human knees, shoulders, elbows, fingers, eyes and wrists.

The discovery of the unusual dielectric properties of a number of simple mixed oxides which crystallize with the perovskite structure in early 1940's lead to a new era of ferroelectric ceramics industries. Ferroelecrtic oxide ceramics are used in a very broad range of functional ceramics and form the materials base for the many electronic applications. These electronic applications accounted for more than 60% of the total high technology ceramics market worldwide in 1990 itself. From then the development in the electro-ceramics field is continuously increasing promoting growth of electro-ceramic industries.

1.2 History and development of ferroelectric materials

The history of ferroelectrics goes back to Rochelle salt or Signette salt (Sodium Potassium tartrate tetrahydrate, $NaKC_4H_4O_6.4H_2O$) which was discovered more than 400 years ago, initially for medicinal purpose. In this material ferroelectric properties were discovered subsequently by Joseph Valasek(1921). The new effect founded by Valasek

was the dielectric hysteresis which was more like ferromagnetic hysteresis loop. It is this analogy with ferromagnetism that ferroelectricity owes its name. Before this discovery, ferroelectricity was only a hypothetical property of solid materials at the turn of the 20^{th} century. However, the practical application of this material was largely limited due to its water solubility. It was after the discovery of ferroelectric ceramics that this class of materials became extremely useful for many applications.

The first ferroelectric ceramic material, which was discovered in mid 1940s, was Barium Titanate ($BaTiO_3$)[1-3]. Before Barium Titanate came into limelight, the widely used dielectric materials were steatite, mica, TiO_2, $MgTiO_3$ and $CaTiO_3$ with dielectric constant $\leq$100. During the World War II, there was pressing needs for high dielectric constant materials to fabricate high capacitance capacitors. Before publications were available in the literature, $BaTiO_3$ has been studied as a high dielectric constant material already. Shortly thereafter, ferroelectricity was reported in this material by Wul and Goldman (1945) [4].

1.3 Dielectrics

Dielectrics are insulating materials, in which the electrons are bounded by their parent atoms/molecules and thus usually they do not contain any free charge carriers for conduction [5]. Even with a small applied voltage or thermal energy at normal temperature, electrons are not free for conduction. However, they do contain positive and negative charges, as usual; which though bound together but can be affected by a strong applied field. In certain dielectric materials the constituent atoms are ionized to a certain degree and contain positively and negatively charged ions which are called Polar Dielectrics. Dielectric materials offer a very high resistance to the passage of charge carriers, in turn electric current, and therefore differ in their basic electrical properties from conductive materials. An applied electric field produces an electric current in a conducting material but in case of dielectrics the applied field causes the redistribution of the charges without removing them from their original atom/molecule. When a sufficient electric field is applied, cations are attracted to the cathode side and anions to the anode

side due to the electrostatic attraction, thereby, forming electric dipoles. A material is said to be polarized when the centre of positive charges do not coincide with that of negative charges and the phenomenon is known as Polarization of the dielectric. Since in general, dielectric materials contain both bound and smaller number of mobile charges, applied electric fields produce both current and polarization.

1.3.1 General Properties of Dielectrics

1.3.1.1 Dielectric Polarization

The most important property of dielectrics is that they tend to polarize under the effect of external electric field. The phenomenon of polarization leads to the alignment of the dipoles of the dielectric and it acquires an *electric dipole moment* **p** [6]. From a macroscopic point of view, the negative charges of the dielectric material are displaced relative to the positive charges and the material is said to be polarized [7].

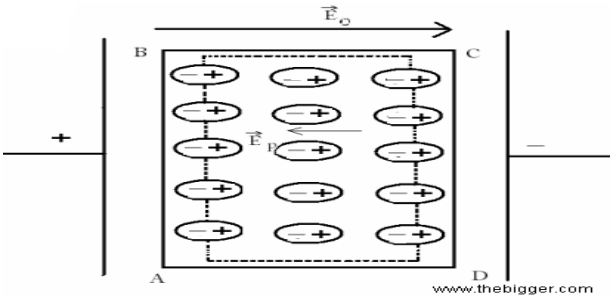

Fig. 1.1: Dielectric polarization

The state of dielectric on which an external electric field is applied can be explained by the use of two vector quantities: intensity of the *applied electric field* E and the *polarization vector* P. The magnitude of polarization P of a dielectric numerically describes the external electric field each volume of the dielectric has no electric dipole moment as the algebraic sum of the dipole moment within each volume element of the dielectric due to the contributing dipoles is equal to zero because of the random orientation of the dipoles. The external electric field forces the charges to orient themselves into a certain ordered arrangement in the direction of the applied field, as is

schematically shown in Fig 1.1. In such a case each volume element of dielectric will have an dipole moment other than zero and equal to the vector sum **Σp** of the moments of all the polarized molecules present in this volume element. The polarization P can be expressed quantitatively as the sum of the electric dipole moment per unit volume,

$$\mathbf{P = \Sigma p / V} \qquad \mathbf{(1.1)}$$

Apart from the vector quantities **P** and **E** discussed above, the macroscopic behavior under static or low frequency conditions, can also be described by another vector quantity-electric displacement vector **D.**

Dielectric capacitors can hold more electric charge as compared to the air-filled capacitors because of the charge holding capacity of the dielectrics due to dielectric polarization **P.** The physical quantity corresponding to the stored charge per unit area is called the electric displacement D and is related to the electric field E by the following expressions [8]:

$$\mathbf{D = \epsilon_r \epsilon_o E} \qquad \mathbf{(1.2)}$$

$$\mathbf{D = \epsilon_o E + P} \qquad \mathbf{(1.3)}$$

On comparing Eqs. (1.2) and (1.3), we get the relation between P and E for an isotropic material as:

$$\mathbf{P = \epsilon_o(\epsilon_r - 1)\, E = \epsilon_o \chi_e E} \qquad \mathbf{(1.4)}$$

where ϵ_o is the permittivity of the free space and ϵ_r is the relative permittivity. The quantity $(\epsilon_r - 1)$ is known as the electrical or dielectric susceptibility χ_e.

Permittivity is a macroscopic description of the properties of the dielectric [9]. In order to understand what is happening inside the dielectric material when an external electric field is applied, we have to link the permittivity of the material to atomic/molecular mechanism so as to describe the process of polarization [9].The polarization has been used to represent the bound charges at the surface of the material. If the polarizing entities in the in a solid are close enough to each other, the field component due to induced polarization can help produce dipoles [7]. The induced field depends on the

actual field experienced by the individual atom/molecule which is different from the actual applied field **E** [10]. As shown in Fig. 1.2, the field is not constant as we move through the dielectric because its value depends not only on the applied field but also on the orientation of the nearby dipoles. Therefore, the actual field experienced by a molecule in a dielectric is the local field $\mathbf{E_{loc}}$. Hence, the polarization described by the mathematical equation (1.4) is proportional to the $\mathbf{E_{loc}}$ at the site of polarizing entity [7] and is expressed as:

$$\mathbf{P=\epsilon_o \chi_e E_{loc}} \qquad \mathbf{(1.5)}$$

The simplest case that illustrates this important concept is that of a spherical specimen of a crystal having a simple cubic lattice; the local field $\mathbf{E_{loc}}$ acting on a molecule increases with the polarization as [10]:

$$\mathbf{E_{loc}=E+P/3\epsilon_o} \qquad \mathbf{(1.6)}$$

The induced polarization in the molecule not only depends on this local field $\mathbf{E_{loc}}$ rather than the average or applied field **E.** Thus,

$$\mathbf{P_{induced}=\alpha E_{loc}} \qquad \mathbf{(1.7)}$$

where the constant α is called the polarizability. Thus, the polarizability of an atom is the ratio of the average dipole moment induced in a unit volume of the dielectric to the effective local field.

1.3.1.2 Types of Polarization

In general, there are four types of polarization which contribute to the dielectric characteristic [11]:

(i) **Electronic Polarization (α_e):** It occurs in all the dielectric materials. It is mainly due to the displacement of the negatively charged electrons with respect to the positively charged core. The electronic polarizability α_e is proportional to the radius of the atom/molecule [8]. In general, electronic polarization is independent of the temperature.

(ii) **Ionic Polarization (α_i):** This type of polarization occurs in the material having ionic

bond between two dissimilar atoms eg. NaCl. In this the center of positive ions and negative ions get displaced under the effect of applied field. The ionic polarization is also independent of the temperature.

(iii**) Orientation Polarization (α_o):** It is mainly due to the alignment of permanent dipoles. At room temperature, all dipole moments have statistical distributions of their directions [12]. An electric field generates a preferred direction for the dipoles, while the thermal movement of the atoms disturbs the alignment. It is temperature dependent.

(iv) **Space charge Polarization (α_s):** This type of polarization occurs mainly due to lattice vacancy in dielectrics. The effect of this will be localized accumulation of charge which will induce its image charge on an electrode and give rise to dipole moment.

The total polarization of a dielectric material is due to the contribution of all the polarizations. So, the total polarizability is the sum total of all the polarizations:

$$\alpha=\alpha_e+\alpha_i+\alpha_o+\alpha_s \qquad (1.8)$$

where α represent total polarization.

The dispersion of the dielectric response of each type leads to dielectric losses which can mathematically expressed by a complex dielectric permittivity:

$$\epsilon=\epsilon_r'-j\epsilon_r'' \qquad (1.9)$$

Dielectric losses are usually described by the loss tangent given by

$$\tan\delta=\epsilon_r''/\epsilon_r' \qquad (1.10)$$

1.4 Ferroelectricity

Ferroelectricity, property of certain non-conducting, or dielectrics, which possess spontaneous electric polarization that can be can be reversed by the application of an appropriate external electric field. Basically, ferroelectric is a subclass of polar crystals whose electric dipoles can be reversed in direction by the application of external electric

field.

The ferroelectric properties in a given material ceases above a characteristic temperature, called Curie Temperature (T_c), because the heat agitates the dipole sufficiently to overcome the forces that spontaneously align them. Above Curie temperature, the material becomes paraelectric and thus material undergoes a phase transition. The ferroelectric structure has low crystal symmetry than paraelectric (non-polarized) state; hence a change in crystal structure has been observed at transition temperature.

1.4.1 General Properties of ferroelectrics

1.4.1.1 Crystal symmetry

The thousands of crystals in nature can all be grouped together into 230 microscopic symmetry types or space groups based on the symmetry elements. A combination of these symmetry elements gives us the macroscopic symmetry also called as point groups. Out of the 230 space groups there are just 32 point groups. The 32 point groups can be further classified into: (i) one with the centre of symmetry i.e. (i) centrosymmetric (ii) one with the lack of centre of symmetry i.e. non-centrosymmetric.

The centrosymmetric point groups do not possess polar properties whereas the non-centrosymmetric possess one or more polar axes. Of these, 20 classes are piezoelectric which possess the property that the application of mechanical stress will induce polarization in them and vice-versa. Out of these 20 piezoelectrics, 10 have a unique polar axis which implies that they are spontaneously polarized. Crystals belonging to these 10 classes are called pyroelectric because polarization varies with temperature. The ferroelectric crystals belong to the pyroelectric family. Hence, ferroelectrics exhibit two properties: presence of spontaneous polarization and its reversibility with the applied field.

1.4.1.2 Spontaneous polarization and pyroelectric effect

The spontaneous polarization is given by the value of the dipole moment per unit volume. The axis of spontaneous polarization is usually along a given crystal axis. Though

a crystal with polar axes (twenty non-centrosymmetric point groups) shows the piezoelectric effect, it is not compulsory for it to have a spontaneous polarization vector. It could be due to the canceling of the electric moments along the different polar axes to give a zero net polarization. Only crystals with a unique polar axis (10 out of 21 non-centrosymmetric point groups) show a spontaneous polarization vector $\mathbf{P_s}$ along this axis. The value of the spontaneous polarization depends on the temperature. This is called the pyroelectric effect which was first discovered in tourmaline by Teophrast in 314 B.C. and named by Brewster in 1824 [13]. The pyroelectric effect can be described by the pyroelectric coefficient, $\prod$. A small change in the temperature ΔT, in a crystal, leads to a change in the spontaneous polarization vector $\Delta \mathbf{P_s}$ given by,

$$\Delta \mathbf{P_s} = \prod (\Delta \mathbf{T})^3 \qquad \textbf{(1.11)}$$

Pyroelectric crystals show spontaneous polarization in a particular temperature range. If the spontaneous polarization of such crystals can be reversed by applying some external electric field, such crystals are called as Ferroelectrics. Therefore, all crystals which show ferroelectric behavior are pyroelectrics but vice-versa is not true.

1.4.1.3 Ferroelectric domain and hysteresis loop

Ferroelectric crystals possess small regions with uniform and unidirectional electric dipoles called ferroelectric domains. All the dipoles within a domain are directed in the same direction, thereby, a domain has a net polarization. There may be many domains in a crystal which are separated by what we call domain walls. The orientation of different domains may be in different directions, thereby, causing a net zero polarization of the ferroelectric crystal in the absence of external field. Although the polarization within a domain can be reversed by applying external field which is called as domain switching [14,15].

The main difference between pyroelectic and ferroelectric materials is that the direction of spontaneous polarization cab be reversed by the application of external field. The polarization reversal can be observed by measuring the ferroelectric hysteresis as shown in Fig. 1.3. As the electric field strength is increased, the domains start to align in the positive direction giving rise to a rapid increase in the polarization (OB). At very high

field, the polarization reaches a saturation point (P_{sat}). When the electric field is removed, the polarization does not reduce to zero. This polarization (when applied electric field reduces to zero) is called as Remanent Polarization P_r. The crystal get completely depolarized when a field of magnitude OF is applied in the reverse direction. This field is known as Coercive Field strength E_c. If the field is further increased in the reverse direction, the direction of polarization also reverses and a hysteresis loop is obtained. The value of Spontaneous Polarization P_s (OE) is obtained by extrapolating the curve onto the polarization axes (CE).

1.4.1.4 Curie Temperature and Phase Transition

All ferroelectric materials exhibit a transition temperature called the Curie Temperature (T_c). At a temperature $T \geq T_c$, the crystal does not show ferroelectricity, while for $T < T_c$, it is ferroelectric. On increasing the temperature through the Curie point, a ferroelectric crystal undergoes a phase transition from a ferroelectric phase to a non-ferroelectric phase. If there are more than one ferroelectric phases, the temperature at which the crystal transforms from one ferroelectric phase to another is called the transition temperature. Near the Curie point or transition temperatures, thermodynamic properties including dielectric, elastic, optical, and thermal constants show abnormal behavior. This is due to a distortion in the crystal as the phase changes. The temperature dependence of the dielectric constant above the Curie point ($T > T_c$) in ferroelectric crystals is governed by the Curie-Weiss law :

$$\epsilon = \epsilon_o + C/(T - T_o) \qquad (1.12)$$

where c is a constant called Curie constant and T_o is the Curie Temperature, ϵ is the permittivity of the materials and ϵ_o s the permittivity of the free space. The curie temperature T_o is different from the curie point T_c.

1.4.2 Classification of ferroelectric materials

Ferroelectric materials can be classified on the basis of:

(a) The mechanism of the appearance of spontaneous polarization

(b) The crystal structure

(a)The mechanism of the appearance of spontaneous polarization

There are two mechanism under this category as discussed below.

(i) Displacive type

In this case, spontaneous polarization is produced due to the displacement of certain ions which causes a rearrangement of the structure. The direction of the polarization coincides with the direction of the displacements. The polarization of this type of ferroelectrics is usually associated with the displacement of a cation from the centre of the surrounding oxygen octahedron. Depending on the geometry of the structure, the nature of the binding and the electronic configuration of the atoms, the resulting dipole moments are oriented either parallel or anti-parallel in a given structure. Most of the oxide ferroelectric fall in this category.

(ii) Order-disorder type

Certain ferroelectrics exhibit a transition which involves the ordering of certain structure elements which were disordered before the transition. The polarization in these takes place in two stages: appearance of dipoles because of deformation of the atomic groups and the alignment of dipole due to the ordering of the structural elements.

(b) The crystal structure

On the basis of the crystal structure they are mainly classified into four subcategories:

(i) Perovskite group

Perovskite is a family name of a group of materials and the mineral name of Calcium Titanate (CaTiO3) having a structure of the type ABO_3 (Fig1.2). Many piezoelectric (which includes ferroelectrics) ceramics such as Barium Titanate ($BaTiO_3$), Lead Titanate ($PbTiO_3$), Lead Lanthanum Zirconate Titanate(PLZT) have a perovskite type structure.

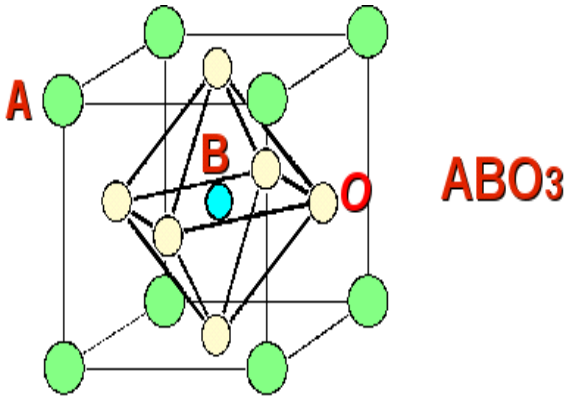

Fig. 1.2: Perovskites type crystal structure.

(ii) Tungsten-Bronze group

The tungsten bronze type ferroelectric crystals have a structure similar to tetragonal tungsten bronze K_xWO_3 (x<1). Lead niobate ($PbNb_2O_6$) was one of the first crystals of the tungsten bronze type structure to show useful ferroelectric properties. Fig. 1.3 shows the tungsten bronze type structure. The open nature of the structure allows a wide range of substitution at the site of cation and anion without the loss of ferroelectricity [16].

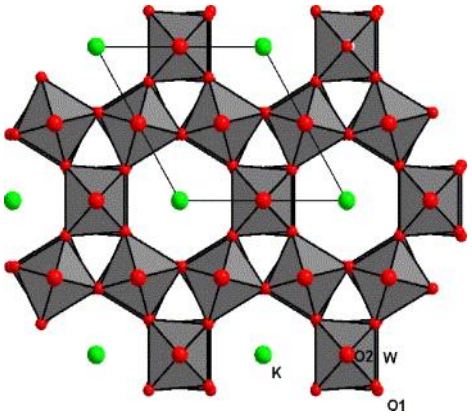

Fig. 1.3: Projection of the tungsten-bronze crystal structure.

(iii) Bismuth Oxide Layer Structure group

The two most important piezoelectric materials containing $(Bi_2O_2)^{2+}$ layer are Bismuth Titanate ($Bi_4Ti_3O_{12}$) and lead bismuth niobate ($PbBi_2Nb_2O_9$). As shown in Fig. 1.6, the structure consists of corner linked perovskite-like sheets, separated by $(Bi_2O_2)^{2+}$ layers [17]. The plate like crystal structure of these compounds leads to highly anisotropic ferroelectric properties. The bismuth oxide layer structured ferroelectrics may become important piezoelectric ceramics because of their stability, higher operating temperature and higher operating frequency.

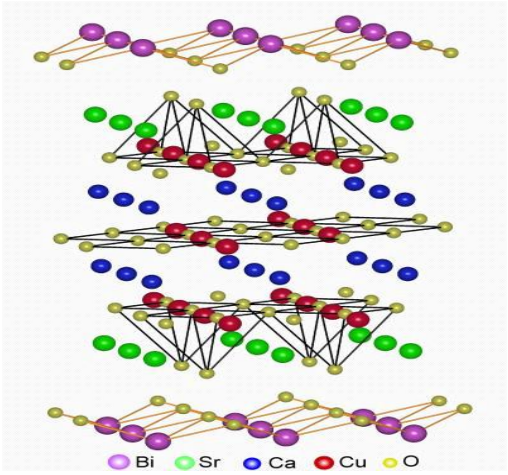

Fig. 1.4: Crystal structure of Bismuth oxide layer structured (BLSF) ferroelectric compounds

(iv) Pyrochlore group

Members of this group have the general formula $A_2B_2O_7$ and the crystal structure is shown in Fig. 1.5. The A-site can be represented by any of a long list of metal ions: lead, calcium, potassium, bismuth, sodium, barium, cadmium, cerium etc. While the B-site can be represented by any of these metal ions: niobium, tungsten, tantalum, titanium etc. $Cd_2Nb_2O_7$, $Y_2Ti_2O_7$, $Mn_2Sb_2O_7$ etc. belong to this family.

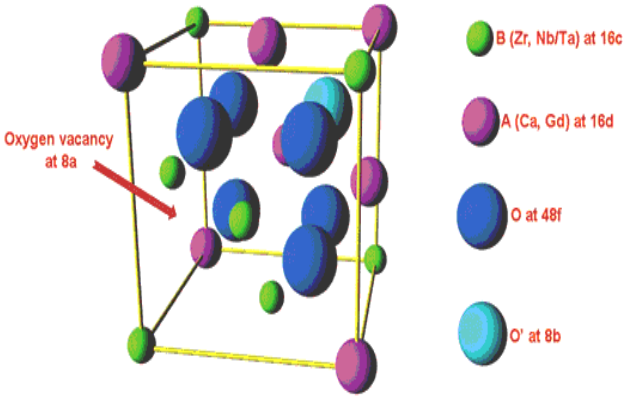

Fig. 1.5: Crystal structure of pyrochlore group.

1.5 Crystal Structure of $BaTiO_3$

It is a ternary compound of the formula ABO_3 such that A and B differ in size. It is an FCC-derivative structure in which larger cation A and oxygen together form an FCC-lattice while smaller cation B occupies the octahedral interstitial sites in the FCC array. The structure is a network of corner-linked oxygen octahedra, with the smaller cation filling the octahedral holes and the large cation filling the dodecahedral holes. The unit cell is shown in Fig. 1.6.

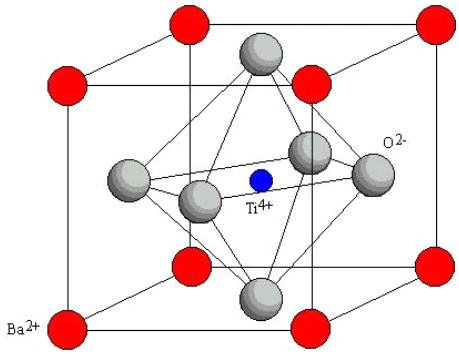

Fig. 1.6: Crystal structure of Barium Titanate.

The coordination number of A (Ba^{+2}) is 12, while the coordination number of B (Ti^{+4}) is 6. So, Barium Titanate provide the scope for substitution of cations at the A-site

or B-site, as well as the anions, but the substitution must maintain charge balance and size should be maintained within the range for particular coordination number [19]. The substitution at either site by appropriate element would help to tailor the properties of Barium Titanate.

1.6 Motivation and aim of the present work

The perovskite family includes many titanates used in various electroceramic applications, for example, mulitilayer ceramic capacitors (MLCC) electronic, electro-optical and electromechanical applications of ceramics. The uses for these materials are based upon their intrinsic dielectric, ferroelectric, piezoelectric and pyroelectric properties of relevance in corresponding applications.

The perovskite structured Barium Titanate is an important ferroelectric material and therefore has been a progressive area of research for many years [18]. The electrical properties, ferroelectric properties of Barium Titanate may be efficiently controlled by doping with transition elements. Barium Titanate has two sites where substitution can be done maintaining the charge balance and size, A-site and B-site. Doping of either A-site ions or B-site ions modifies the Curie temperature (T_c) and the nature of ferroelectric to paraelectric transition in Barium Titanate. The substitution at either site show different change in the properties.

The structural and dielectric properties of ferroelectric materials are also influenced by their particle size. With the miniaturization of electronic devices, it becomes very important to investigate the particle size effects on ferroelectric properties of $BaTiO_3$. The particle size plays an important role in phase transition and dielectric properties.

After extensive literature survey, it has been realized that although, some work has been reported for both A-site as well as B-site substitution but a detailed study of changes in properties due to substitution and size of the particles is lacking. With this purpose, the changes in dielectric and ferroelectric properties of Iron incorporated BT and particle size dependency of the properties has been investigated. Present investigation is focused on the

influence of B-site substitution on dielectric properties of Barium Titanate. Moreover, the effect of sintering temperature on the electrical properties has been studied.

The results and discussions of the studies carried out are discussed in further chapters. The details of the sample preparation techniques and characterization techniques used in the course are discussed in detail in **Chapter 2.**

Chapter 3 contains the effect of the Iron substitution at Titanium site, optimization of the milling duration and sintering temperature of the Iron substituted Barium Titanate.

In **Chapter 4**, the results obtained have been concluded and scope for future work has been discussed.

REFERENCES

[1] G. H. Haertling, J. Am. Ceram. Soc. **82** (1999) 797.

[2] D. Damjanovic, Rep. Prog. Physics **61** (1998) 1267.

[3] L. E. Cross and R. E. Newnham, *History of ferroelectrics, ceramics and civilization. High Technology ceramics-past, present and future,* vol. III (American Ceramic Society, Westerville, Ohio,1987) p. 289-305.

[4] B. M. Wul and I. M. Goldman, Dokl. Akad. Nauk. SSSR **46** (1945) 154.

[5] D. Baker, D. C. Koehler, W. O. Fleckenstein, G. E. Roden and R. Sabia, *Materials Technology,* Vol. II (Prentice-Hall Inc. Englewod Cliffs, New Jersey).

[6] B. Tareev, *Physics of Dielectric Materials* (Mir Publishers, Moscow, 1979).

[7] R. A. Conclaser and S. D. Nagle, Materials and Devices foe Electrical Engineers and Physicists (McGraw Hill Co., New York)

[8] R. C. Buchanan, *Ceramic Materials for Electronics: Procesing, Properties & Applications*, (Marcel Dekker Inc., New York, 2002).

[9] J. C. Anderson and K. D. Leaver, Materials Science (Thomas Nelson and Sons Ltd., London. 1969).

[10] S. O. Kasap, *Principles of Electronic Materials and Devices,* 2nd Edition (Tata McGraw Hill Co., New York).

[11] C. Kittel, *Introduction to Solid State Physics* (John Wiley and Sons Inc., New Jersey, 7th Edition, 1996).

[12] R. Waser, U. Bottger and S.Tiedke, *Polar Oxides: Properties, Characterization and Imaging* (Wiley-VCH Verlag GmbH & Co. KGaA, Weinheim, 2005).

[13] R. M. Rose, L. A. Shepard and J. Wulff, *Electronic Proeprties* (Wiley Eastern Pvt.

Ltd., North Dakota, 1965).

[14] B. T. Batthais and A. V. Hippel, Phys. Rev. **73** (1948) 1378.

[15] A. V. Hippel, Rev. Modern Phys. **22** (1950) 221.

[16] Y. H. Xu, *Ferroelectric Materials* and their Applications (Elsevier Science Publishers, Amsterdam, 1991).

[17] B. Aurivillius, Ark. Kemi. **2**(1950) 519.

[18] A. Jana, T. K. Kundu, S. K. Pradhan and D. Chaksavorty, J. of App. Phys. **97** (2005) 044311.

[19] Daniel Popovici, Masanori Okuyama and Jun Akedo, National Institute of Advanced Industrial Science and Technology, Osaka University, Japan.

Chapter 2

Experimental Details

This chapter contains the experimental details along with the theoretical background of the various structural and electrical parameters studied in the present work. The experimental techniques including the procedure for the sample preparation and characterization are described.

2.1 Preparation Techniques

The following section discusses the method for the preparation of the samples. The samples can be prepared by two methods.

(i) Solid-State Reaction Method

(ii) Mechanical Activation Method

2.1.1 Solid-State Reaction Method

High purity raw materials (carbonates and oxides) which are in powdered form are first weighed according to their stoichiometric formula of the composition. The particle size should be in submicron for the reaction to occur. The powders are mixed and grinded. The powder mixture is kept for calcinations at proper temperature. Calcination helps in the decomposition of the constituent carbonates into oxides and removal of carbon dioxide. For example:

$$BaCO_3 \longrightarrow BaO + CO_2$$

During the calcinations step, the reaction takes place between the constituents resulting in the partial development of the phase [1,2]. The calcinations temperature is

important as it affects the final product and structure. After calcinations, the mixture is thoroughly grounded. Then, an organic binder like Polyvinyl alcohol (PVA) is added for sufficient adhesion during pellet formation. There are various shaping methods like powder compaction/ dry pressing, isotatic pressing, extraction, slip-casting etc. [3]. The choice of method depends on the type of material used, desired shape and thickness of product. After making pellets, they are kept for sintering. During sintering, particles join in the region of contact by growth of neck [4,5]. Therefore, it results in densification and grain growth. The sintering process considerably effects grain boundaries and pores. The sintering process have been explained by many models and mechanisms [6,7,8]. From the matter transport point of view, sintering process can be divided in to three stages, viz., initial stage, intermediate stage and final stage. The initial stage is linked with the growth of neck between the particles by lattice diffusion. In the intermediate stage, the structure grows and the particles lose their individual identity, the pores form continuous channel and all the pores intersect at the grain boundaries. At the final stage, grains occur as either isolated entities at grain corner or totally enfold within them. Thus, the sintering temperature and the duration are crucial and should be optimized. Thereafter, the pellets are polished and electrode to provide electrical contacts.

2.1.2 Mechanical Activation Method

In mechanical activation method, the reaction between the oxides is activated by milling the powder (mixture of constituents) which produces a high mechanical energy. This process skips the high energy consuming calcinations step, making the preparation simpler than the conventional solid-state reaction technique discussed earlier. In the mechanical activation method, the need for calcination of sample at a very high temperature is avoided and thus the requirement of very high temperature furnace is omitted. In this method, the stoichiometric mixture of powders was milled in a planetary ball mill (Retsch-PM 100, Germany)

Sample preparation

This section presents the details of the method used for the preparation of the various compositions studied in the present work. First sample was prepared by mixing Barium

Carbonate ($BaCO_3$), Titanium Oxide (TiO_2) in stoichiometric composition. The mixture was milled for 5 hrs in ball milling at a speed of 300 rpm. Then the mixture was calcined at 150^oC. The powder was mixed with 3 wt% Polyvinyl alcohol as binder and then grinded uniformly to mix it. The disk shaped pellets of the prepared samples were made by pressing at 350 MPa. The next set of samples was prepared by mixing Barium Carbonate ($BaCO_3$), Titanium Oxide (TiO_2) and Ferrous oxide (Fe_2O_3). To optimize the milling duration the powders were milled for 5 hrs, 10 hrs and 15 hrs at a milling speed of 300 rpm. Milling was carried out in toluene medium with 10 mm diameter stainless steel balls in stainless steel vial with a ball-to-powder ration of 8:1. The milling was stopped after every 1 hour for 30 minutes in order to cool down the system. The mixture was then calcined at 150^o C to remove the toluene from the powder. The samples was then mixed with 3 wt% Polyvinyl alcohol as binder and then grinded to uniformly mix the binder. Then, to make pellets, the powder is weighed and pressed at 350 MPa into a disk shaped pellet. To determine the optimum sintering condition, the sample was sintered in air at the following sintering conditions:

(i) 950^oC; soaking period of 3 hrs

(ii) 1150^oC; soaking period of 3 hrs

High temperature conductive silver paste was applied over the parallel surfaces of the samples which act as electrodes and were cured at 350^oC for 1 hour. The ferroelectric ceramic having the composition $BaTi_{0.95}Fe_{0.05}O_3$ have been prepared.

2.2 Characterization Techniques

The following section discusses the instruments / techniques used for the structural and electrical characterization of the samples.

2.2.1 Structural characterization

2.2.1.1 X-Ray diffraction (XRD)

X-ray crystallography helps us in determining the crystallinity, orientation of the plane and crystallite size within a single crystal. X-ray crystallography is a technique in which the pattern produced by the diffraction of x-rays through the closely spaced lattice of atoms in a crystal is recorded and then analyzed to reveal the nature of that lattice. Diffraction occurs as waves interact with a regular structure whose interplanery distance is of some order of the wavelength of the x-rays. When the interplaner distance is of the order of the wavelength of x-rays, X-rays scattered from a crystalline solid can constructively interfere, producing a diffracted beam. In order to interfere the beams constructively, they must follow the Bragg's Law:

$$n\lambda=2d\sin\theta \qquad (2.1)$$

X-ray powder diffraction finds frequent use in materials science as it is non-destructive and easy to use.

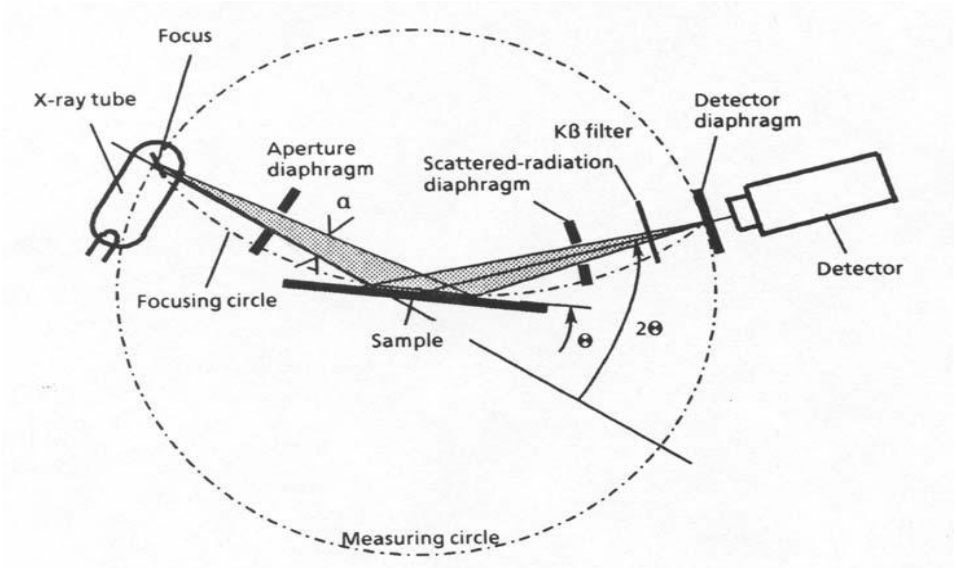

(a)

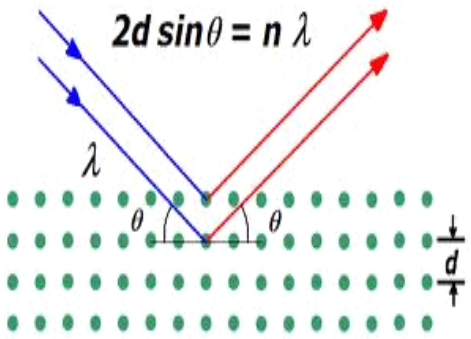

(b)

Fig. 2.1:(a) Schematic diagram of X-ray Powder Diffraction (θ-2θ mode)

(b) Diagram of Bragg's Diffraction Law

1. X-Ray analysis

(a) *Phase Identification*

The most widespread use of this technique is the phase indentification of crystalline solids. Each crystalline solid produces its own characteristic diffraction pattern. General phase/composition identification of the major, minor and the compound present in the sample by comparing the observed diffraction pattern to a database like JCPDS (Joint Committee of Powder Diffraction Standards). The positions and the intensity of the lines are the characteristic of that particular phase and the pattern thus provides the fingerprint of the materials.

(b) *Crystallinity*

The crystalline solid produces a diffraction pattern which consists of a series of sharp peaks, whereas the amorphous materials produce a broad background signal. So, XRD can be used to determine the crystallinity by comparing the integrated intensity of the background pattern to that of sharp peaks.

(c) *Crystallite size*

The average crystallite size is determined by using Debye-Scherrer formula:

$$P_{hkl}=k\lambda/\beta\cos\theta \qquad (2.2)$$

where k= 0.89-1.39, λ = wavelength of the used X-rays, β = FWHM (full width at half maxima) and θ = position (angle) of the peak. The broadening of the XRD peak helps in determining the crystallite size. Broader the peak, smaller the crystallite size.

2. X-Ray diffractometer set-up and conditions used

In the present work, X-ray diffraction patterns of all the samples were recorded for the phase analysis to identify the various phases present in the samples. A Bruker (Model D8 Advance) diffractometer as shown in (Fig. 2.2) was used. The X-rays produced are passed through nickel mono-chromator to select only Cu-$K_{\alpha 1}$ radiations with the characteristic wavelength of 1.5405 Angstorm and to remove unwanted wavelengths (Cu-$K_{\alpha 2}$, Cu-$K_{\beta 1}$ etc.). The samples were analyzed in the range from 10^o to 80^o at a scanning rate of 2^o/ min.

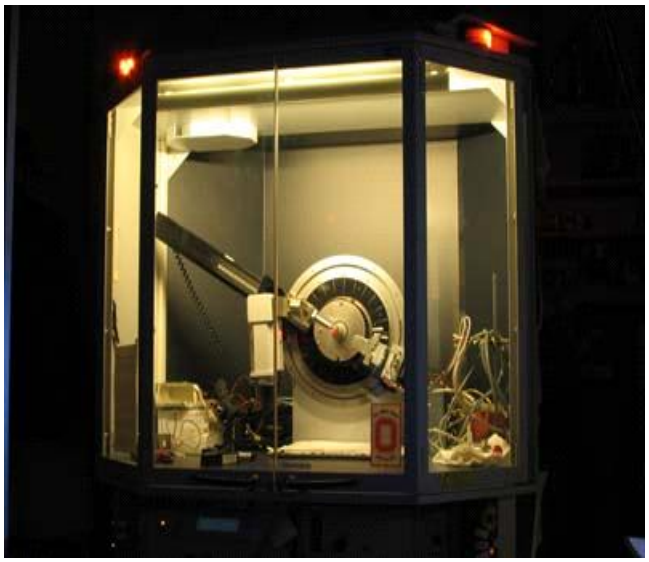

Fig. 2.2: Photograph of used X- ray diffractometer in the Lab.

2.2.1.2 Scanning Electron Microscope

A Scanning Electron Microscope (SEM) is an electron microscope that images a sample by scanning it in raster scan pattern. The SEM uses a focused beam of high energy

electrons to generate a variety of signals at the surface of solid specimens. The signals are obtained from the electron-sample interaction reveal information about the sample including external morphology (texture), chemical composition, and crystalline structure and orientation of the materials making up the sample. It has a large depth of field, which allows a large amount of the sample to be in focus at one time. The images produced are of high resolution and hence the closely spaced features can be examined at a high magnification.

Working Principle of SEM

In a SEM (Fig 2.3), an electron beam is generated thermionically from an electron gun containing a filament (cathode) of Tungsten or Lanthanum Hexaboride (Lab_6). The electron beam is focused using one or two condenser lenses to a spot about 0.4 nm to 5 nm in diameter. The beam passes through pairs of scanning coils which deflect the beam in the x and y axes so that it scans in a raster fashion over a rectangular area of the sample. When the primary electrons interact with the atoms in the sample, the electrons loose energy by repeated random scattering and absorption within the specimen known as the interaction volume. The energy exchange between the electron beam and the sample causes the reflection of high-energy electrons by elastic scattering, emission of secondary electrons by inelastic scattering and emission of electromagnetic radiation. The secondary electrons are detected are detected by specialized detectors. Electronic amplifiers of various types are used to amplify the signals, which are displayed as variations in the brightness over the monitor. The scanning mechanism of monitor is synchronized to that of the beam on the specimen and the resulting image is a distribution of the signal being emitted from the scanned area of the specimen. The image is digitally captured and saved to the computer's hard disc.

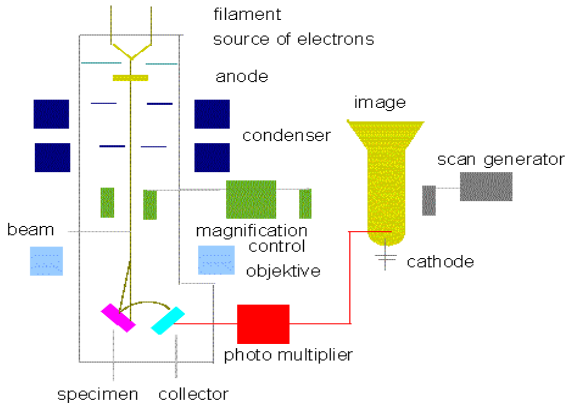

Fig. 2.3: Schematic diagram of SEM

Microstructural studies

In the present work, SEM (Model S-3700N, Hitachi, Japan) is used to find the surface morphology and the average grain size of the samples prepared. The sample is first coated with a thin layer of gold to make its surface conducting. The microstructural images formed by secondary electrons were captured. The parameters of SEM settings used are listed in Table 2.1.

Table 2.1 Typical SEM parameters

Accelerating Voltage	30 kV
Probe Current	40 nA
Working distance	10 mm

2.2.2 Electrical Characterization

2.2.2.1 Dielectric studies

In this class of materials the dielectric constant and dielectric loss are the two most important parameters and studies of the dielectric properties provide a lot of information for understanding the behavior and mechanism of electric polarization [9-11]. Dielectric measurements are mostly used for the identification of the phase transition. As these

materials polarize quickly which is important for their application, it is important to know the frequency dependence of the dielectric behavior.

Capacitance is the ability to hold charge which for a parallel plate capacitor is expressed as:

$$C=\epsilon A/d \qquad (2.3)$$

where A is the area of the plates, d is the distance between the plates and ϵ is the permittivity which is intrinsic property of the dielectric filled between the plates and related to the free space permittivity ϵ_o as:

$$\epsilon=\epsilon_r\epsilon_o \qquad (2.4)$$

where ϵ_r is the relative permittivity.

Complex Permittivity

The response of normal dielectrics to external field usually depends on the frequency of the field. This dependency on the frequency reflects that the dielectric does not respond to the external field instantaneously. That's why, permittivity is often treated as a complex function of the angular frequency (ω) of the applied field and is expressed as:

$$\epsilon_r^*(\omega)=\epsilon_r'(\omega)-j\epsilon_r''(\omega) \qquad (2.5)$$

where $\epsilon_r'(\omega)$ is the real part of the permittivity representing the lossless permittivity which is related to the electrical energy stored within the medium and is known as dielectric constant while $\epsilon_r''(\omega)$ is the imaginary part of the permittivity related to the loss of energy within the medium.

Frequency dependence of permittivity

The total polarization P, the total polarizability α and the relative permittivity ϵ_r in an alternating field all depend on the ease with which the dipoles can reverse alignment with each reversal of the applied electric field [12]. The dependence of ϵ_r on frequency is known as dielectric dispersion. The different polarization mechanisms dominate in different frequency ranges as shown in Fig.2.4

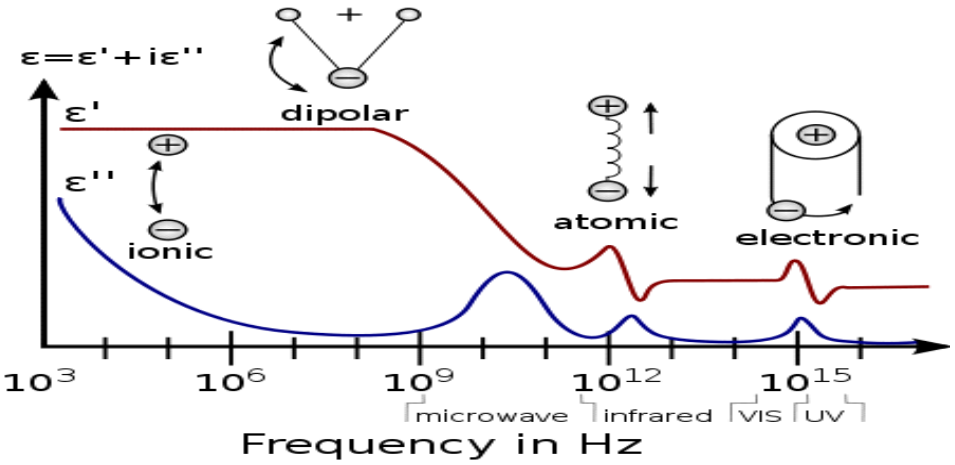

Fig. 2.4: Frequency dependence of real and imaginary part of dielectric constant.

Since the relaxation frequencies of all the four polarization processes differ, it is possible to separate their contributions experimentally. Each polarization component has a characteristic relaxation frequency. The contribution from the slower component decreases as frequency increases. The dielectric loss factor ϵ_r" (ω) peaks at each characteristic frequency.

Temperature dependence of permittivity

The dielectric constant of ionic and electronic materials is small at low temperatures, but increases with increasing temperature because ion mobility increases with temperature [13]. The total permittivity of normal dielectrics increases with increase in temperature but, in case of ferroelectric materials, the permittivity first increases with increases in temperature and reaches peak at Curie temperature, thereafter, decreases as temperature is increased further. Above the Curie temperature, the dielectric constant follows Curie-Weiss law [14].

Measurement of dielectric parameters

A precision LCR meter (Agilent 4284A, USA) was used for measuring the dielectric constant and dielectric loss in the present work. The frequency dependence of dielectric

permittivity and loss was studied in frequency range 20 Hz- 1 MHz. The temperature dependence of dielectric properties was measured from room temperature to 300^{o}C as a function of signal frequency (10 kHz, 100 kHz and 500 kHz) at oscillation amplitude of 1 V with no DC bias. The variation in dielectric constant and loss tangent with temperature were recorded at constant heating rate of 3^{o}C / minute. The least count of temperature measurement was 5^{o}C. For the measurements, the sample was mounted on a two probe sample holder. The schematic diagram of sample holder is shown in Fig. 2.5.

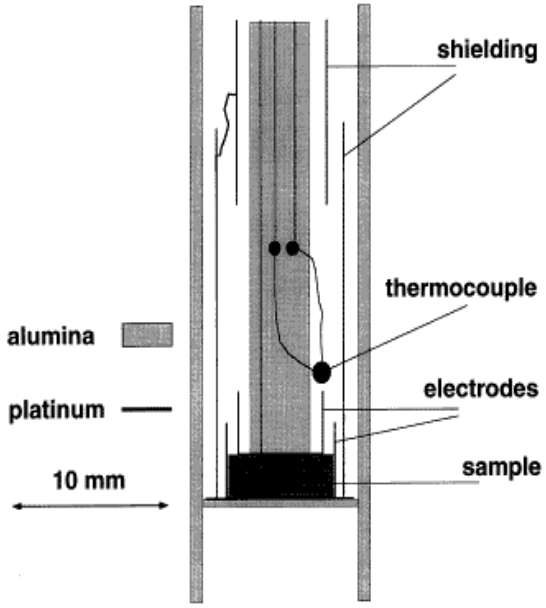

Fig. 2.5: Schematic diagram of the laboratory made sample holder.

2.2.2.2 Electrical Conductivity

Electrical conductivity measures a material's ability to conduct an electric current when an external field is applied across it. Though dielectrics are the materials that do not allow current to flow through them, however, stray charges and defects cause a small conduction through them. The conductivity σ of the dielectrics is extremely small but not zero. In 1926, A. Jaffe [14] put forward the theory that in ionic crystals, conduction can be caused due to ions that tear themselves apart from the lattice points because of thermal oscillations even at low temperatures. This point of view was developed and quantitatively substantiated by Ya Frenkel [15].

The current density in a parallel plate capacitor can be defined in terms of properties of the materials,

$$J=\omega\epsilon_o\epsilon_r''E+j\omega\epsilon_o\epsilon_r'E \quad (2.6)$$

where E is the electric field strength. Thus, we have:

$$J/E=\sigma+j\omega\epsilon_o\epsilon_r' \quad (2.7)$$

which implies that the real part of the ratio J/E is defined as the electrical conductivity σ in the material, i.e.

$$\sigma(\omega)=\omega\epsilon_o\epsilon_r''(\omega) \quad (2.8)$$

The measured loss of material ϵ_r'' can be expressed as a function of both dipolar loss (ϵ_d'') and conductivity (σ) as:

$$\epsilon_r''=\epsilon_d''+\sigma/\omega\epsilon_o \quad (2.9)$$

Mechanisms of electrical conduction in dielectrics

Electrical conduction in dielectrics mainly occur because of either of the three mechanisms discussed below depending on the carrier present in the material [16]:

(i) ***Ionic Conduction*** occurs either through the migration of negative and positive charges under the effect of an external field or through the motion of ions in the vacancies which reflect migration of vacancies.

(ii) ***Molionic Conduction*** occurs through the motion of molecular ions (molions) or groups of ionized molecules. This conduction occurs mainly in amorphous or liquid dielectrics.

(iii) ***Electronic Conduction*** is due to the motion of free charges (electrons and/or holes) in the solid, though the number of free charges in these materials is extremely small.

Thus, electrical conductivity in these materials can involve both electronic and ionic

charge carriers.

Conductivity measurement

The total conductivity (σ_{tot}) of a material is the sum of the dc conductivity (σ_{dc}) and the ac conductivity (σ_{ac}),

$$\sigma_{tot}=\sigma_{dc}+\sigma_{ac}(\omega) \qquad (2.10)$$

The dc conductivity was measured through a high precision electrometer (Keithley 6517A, USA). The measurement was performed at 10V in the temperature range of room temperature to 350^{o} C at a heating rate of 3^{o}C/ minute. Conductivity was calculated using the relation:

$$\sigma_{dc}=d/AR \qquad (2.11)$$

where d is the thickness of the pellet, A is the area of the conducting surface of the pellet and R is the measured resistance of the sample.

The ac conductivity was measured using the relation

$$\sigma(\omega)=\omega\epsilon_{o}\epsilon_{r}'\tan\delta \qquad (2.12)$$

where the dielectric constant (ϵ_r') and the dielectric loss ($\tan\delta$) has already been measured in the dielectric measurement of the sample.

2.2.2.3 Ferroelectric Studies

The observation of hysteresis loop commonly known as Polarization-Electric field (P-E) loop is widely used for the ferroelectric characterization of materials [17]. The P-E loop is obtained using the Sawyer-Tower circuit which is shown in Fig. 2.6.

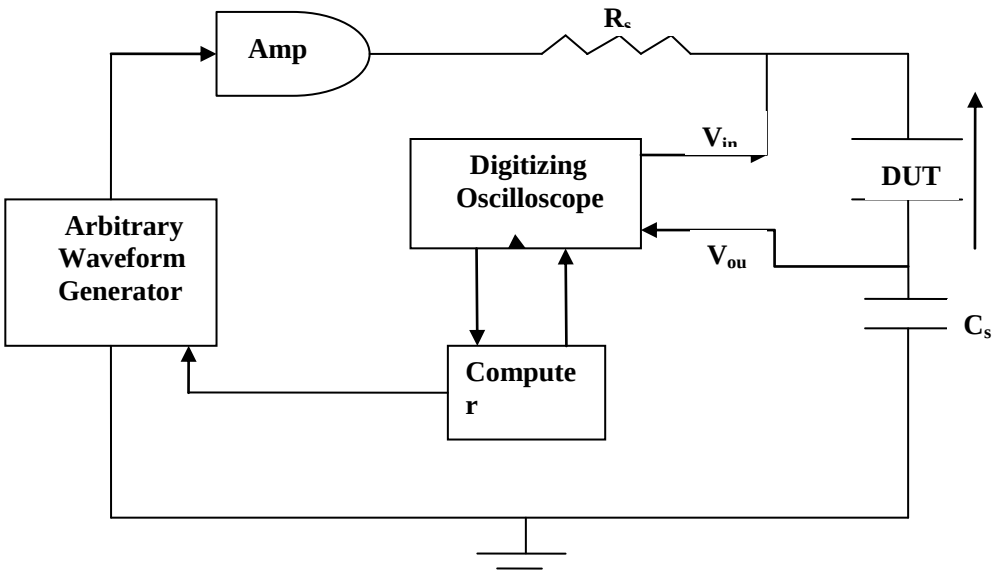

Fig. 2.6: Block Diagram of Sawyer-Tower circuit

The ferroelectric device under test (DUT) is placed in series with a sensing capacitor C_s and a resistor R_s. A computer –controlled waveform generator produces an AC signal, which is applied to the DUT. The voltage at the input and the output of the DUT is measured and is analyzed by the computer (Fig. 2.6). The capacitance of the sensing capacitor must be significantly large than the capacitance of the device under test to minimize its effect on the measurement. The external charge on the sensing capacitor which is proportional to the external charge on the DUT, is calculated from the value of C_s and the voltage measured across C_s,

$$q=C_sV_{out} \qquad (2.13)$$

The voltage applied to the DUT is the difference between the voltage measured at the input and the output of the DUT:

$$V_A=V_{in}-V_{out} \qquad (2.14)$$

The polarization (or charge per unit area) is calculated by dividing the total charge by the area of the pellet. The electric field is calculated by dividing the applied voltage by the thickness of the pellet.

The hysteresis loops were recorded at room temperature (except for few samples where temperature is below room temperature) using an automatic PE- loop tracer based on Sawyer-Tower circuit at a switching frequency of 100 Hz. The device under test i.e. the pellets were placed in silicone oil bath during the measurement. The measurement gives P-E hysteresis loops from which remanent polarization ($2P_r$) and coercive field ($2E_c$) were determined.

References

[1] J. S. Reed and R. B. Runk, *Ceramic Fabrication Processes, Treatise on Materials Science & Technology*, Vol. 9 (Editor F. F. Y. Wang, Academic Press, New York, 1976).

[2] K. G. Ewsuk and L. W. Harrison, *Ceramic Powder Science III, Ceramic Transactions,* Vol. 12 (The American Ceramic Society, Westerville, Ohio, 1990).

[3] D. Baker, D. C. Koehler, W. O. Fleckenstein, G. E. Roden and R. Sabia, *Materials Technology*, Vol. II (Prentice-Hall Inc., Englewood Cliffs, New Jersey).

[4] W. D. Kingery and B. D. Francois, Sintering and Related Phenomena (Gordon Breach Science Publishers, New York, 1965).

[5] K. G. Ewsuk and G. L. Messing, *Hot Isostatic Pressing: Theory and Applications* (ASM International Materials park, Ohio,1991).

[6] D. W. Richerson, *Modern Ceramic Engineering* (Marcel Dekker, New York, 1982).

[7] R. L. Coble and J. E. Burke, *Progress in Ceramic Science,* Vol. 3 (MacMillan, New York, 1963).

[8] N. B. Hannay, *Reactivity of Solids: Treatise on Solid State Chemistry,* Vol. 4 (Plenum Press, New York, 1976).

[9] H. D. Megaw, *Ferroelectricity in crystals* (Methuen & Co. Ltd., London, 1957).

[10] W. Kanzig, *Ferroelectrics and Antiferroelectrics* (Academic Press, New York, 1957).

[11] F. Jona and G. Shirane, Ferroelectric Crystals (Pergamon Press, Oxford, London,

1962).

[12] R. M. Rose, L. A. Shepard and J. Wulff, *Electronic Properties* (Wiley Eastern Pvt. Ltd., New York, 1965).

[13] S. B. Lang, *Source Book of Pyroelectricity* (Gordon & Breach Science Publishers, New York, 1974).

[14] B. Tareev, *Physics of Dielectric Materials* (Mir Publishers, Moscow, 1979).

[15] Y. I. Frenkel, Elecktrichestro (Physics Of Electrets) **8** (1947) 5.

[16] I. Bunget and M. Popenscu, *Physics of Solid Dielectrics* (Elsevier, New York, 1984).

[17] C. B. Sawyer and C. H. Tower, Phys. Rev. **35** (1930) 269.

Chapter 3

Optimization of iron substituted $BaTiO_3$

3.1 Introduction

Barium Titanate is an important ferroelectric material. It is of significant importance due to its lot of applications such as in capacitors, ferroelectric memories and so on. Various application and structural properties of Barium Titanate has already been discussed earlier in section 1.6. There are different techniques to synthesize Barium Titanate [11]. Among these solid state reaction method and mechanical activation method has been preferred to prepare Barium Titanate. The mechanical activation method has reduced the need for high energy consuming calcinations step. The Barium Titanate samples exhibit a ferroelectric to paraelectric phase transition at a particular temperature. The temperature at which this change occurs is called as transition temperature. In this chapter, the results obtained from the Barium Titanate samples have been discussed.

As discussed before, the perovskite structured Barium Titanate samples have two sites for substitution, A-site or B-site substitution [1]. The substitution at either of these sites would lead to change in the properties.

In the present investigation, the subsitution at B-site has been performed and the changes have been observed by optimizing the synthesis conditions of Iron substituted Barium Titanate. Therefore, in this chapter, the processing of ferroelectric powders of Barium Titanate substituted with transition metal (Fe) has been attempted under process parameters such as sintering temperatures and duration of preparation of the sample by mechanical-activation method.

The samples were milled for three different durations and sintered at two different temperatures as discussed in section 2.1.2. The effects of milling duration and sintering temperature on the microstructure, dielectric and ferroelectric property have been

discussed. The optimized condition resulting in high dielectric constant, low dielectric loss and good ferroelectric properties has to be investigated.

3.2 Results of Barium Titanate samples

Barium Titanate samples have been prepared through mechanical activation method. The sample preparation has been discussed in section 2.1.2. The sample of Barium Titanate was characterized so as to analyze it.

3.2.1 Structural Characterization: X-Ray diffraction

The x-ray diffraction pattern of Barium Titanate has been obtained. The diffraction pattern has been shown in Fig 3.1. The peak in the pattern shows that single phase Barium Titanate has been formed. Usually, the peak at 32 degrees depicts the formation of the Barium Titante phase.

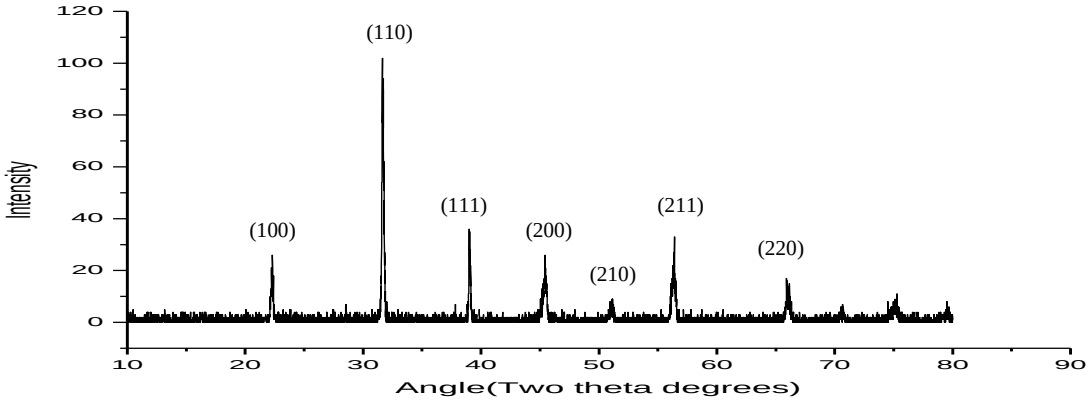

Fig. 3.1: X-ray diffraction pattern of $BaTiO_3$ samples

3.2.2 Electrical Characterization: Dielectric Study

The electrical characterization of the prepared sample has been performed. The variation of dielectric constant with temperature has been obtained for three different frequencies as shown in Fig. 3.2. The frequencies are used in this range because at lower frequencies the dielectric loss is very high leading to no use in applications, whereas the

higher frequencies are not supported by the device used. The peak at about 120^{o}C shows the phase transition i.e. the transition from ferroelectric to paraelectric. The phase transition is very sharp in case of pure Barium Titanate sample. The dielectric pattern obtained for pure Barium Titanate shows the transition from ferroelectric to paraelectric phase at a temperature called the Curie Temperature. The Curie temperature is the same at all the frequencies indicating the non-relaxor behavior of the compound.

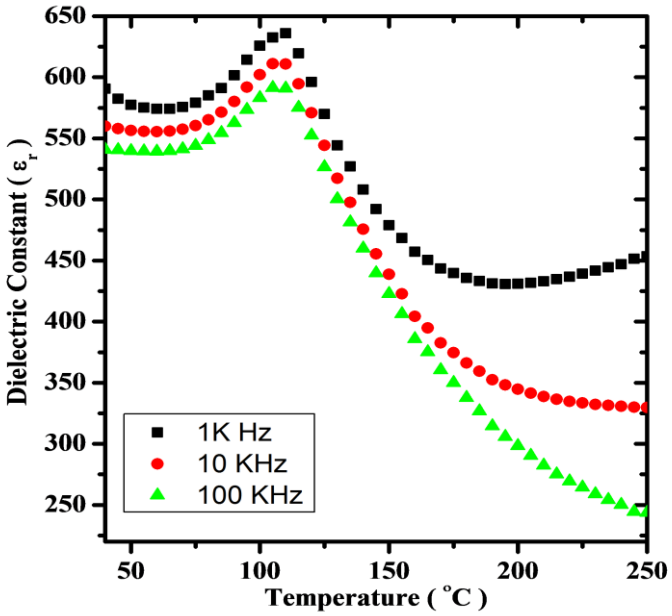

Fig. 3.2: Variation of dielectric constant with temperature.

3.3 Effect of substitution and preparation conditions

The Iron substituted Barium Titanate samples have been prepared as discussed in section 2.1.2. The samples obtained were of the composition of $BaTi_{0.95}Fe_{0.05}O_3$. The sample was milled for three different durations of 5 hrs, 10 hrs and 15 hrs. The milling of sample for different duration may produce particles of different size. This will cause change in the properties of the particles [6]. The samples milled for different durations have been investigated in order to optimize the milling duration. Moreover, the iron

substitution at Ti-site would also cause some changes in the property [7]. The structural and electrical characterization has been studied here in detail here.

3.3.1 Optimization of Milling duration

3.3.1.1 Structural Characterization

3.3.1.1.1 X-ray diffraction

The initial powder was the mixture of constituents in stoichiometric proportions. The samples were milled for 5 hrs, 10 hrs and 15 hrs and calcined at 150^{o}C. Initially, the x-ray diffraction of the powder has been obtained for calcined samples before sintering. The x-ray diffraction pattern of the original powder milled for 5 hrs, 10 hrs and 15 hrs is shown in Fig. 3.3(a), (b) and (c), respectively.

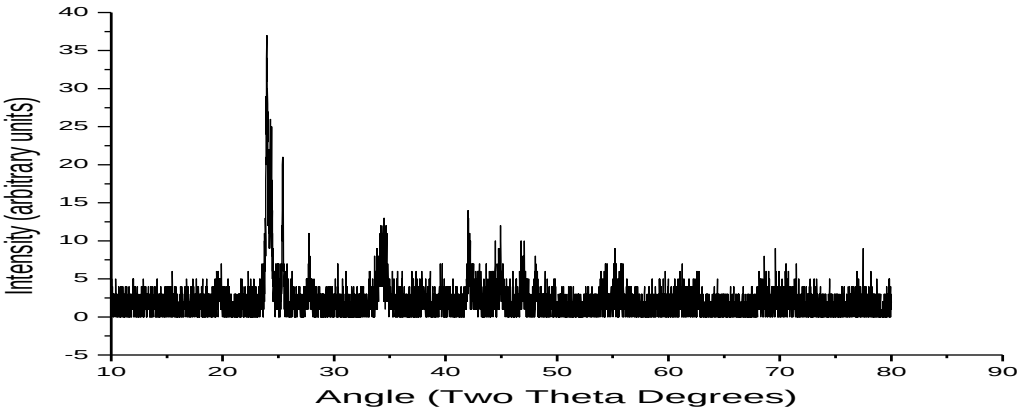

(a)

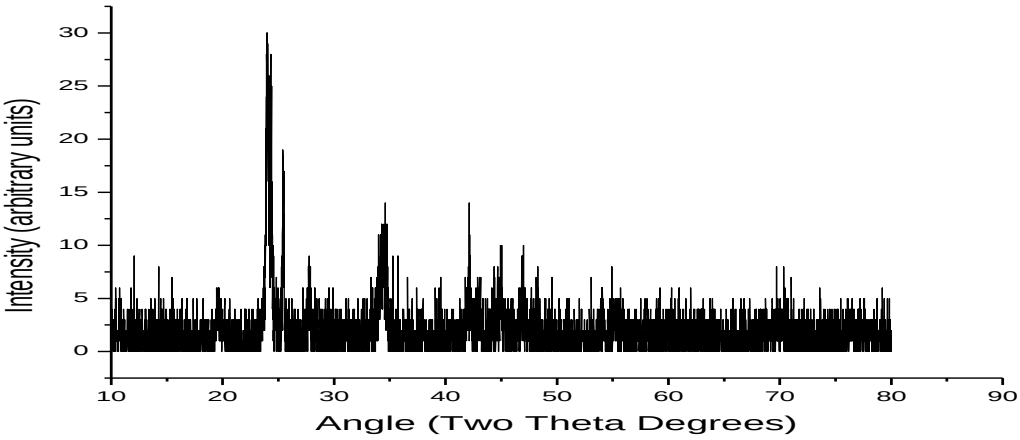

(b)

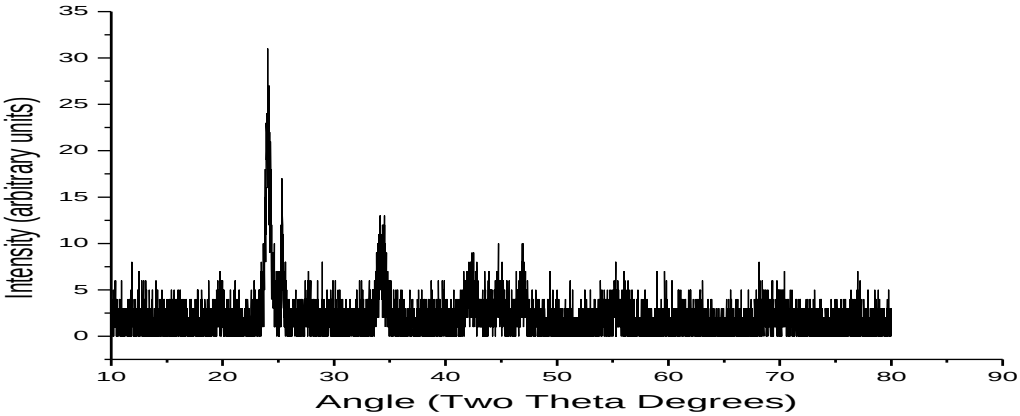

(c)

Fig. 3.3: XRD pattern of the mixture in stoichiometric composition milled for (a) 5 hrs (b) 10 hrs (c) 15 hrs.

It is observed that $BaTiO_3$ has not been formed. The peaks in Barium Titanate samples are generally observed between 30-32.5 (2θ) degrees. But no such peaks has been observed here. Now, the sample is sintered at 950^{o}C for 3 hours. The XRD pattern has been obtained for sintered samples and is shown in Figure 3.4(a), (b) and (c) respectively. The XRD shows the formation of single phase material which shows that iron goes to Ti site instead of formation of impurity peaks.

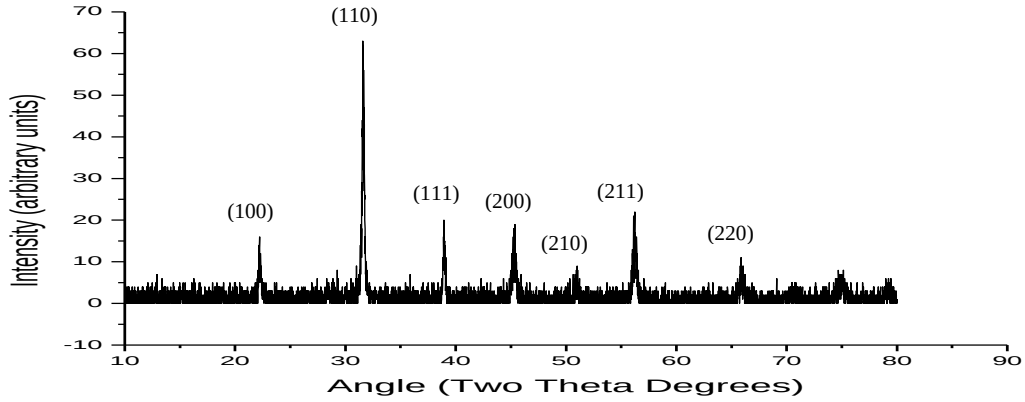

(a)

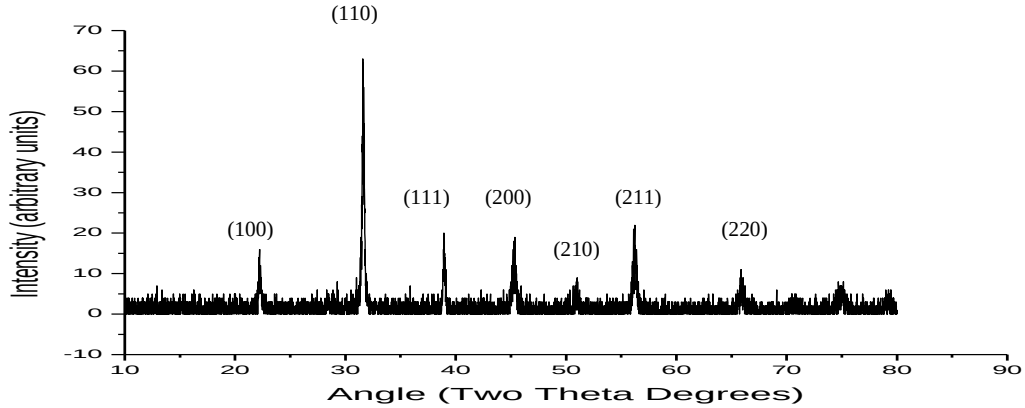

(b)

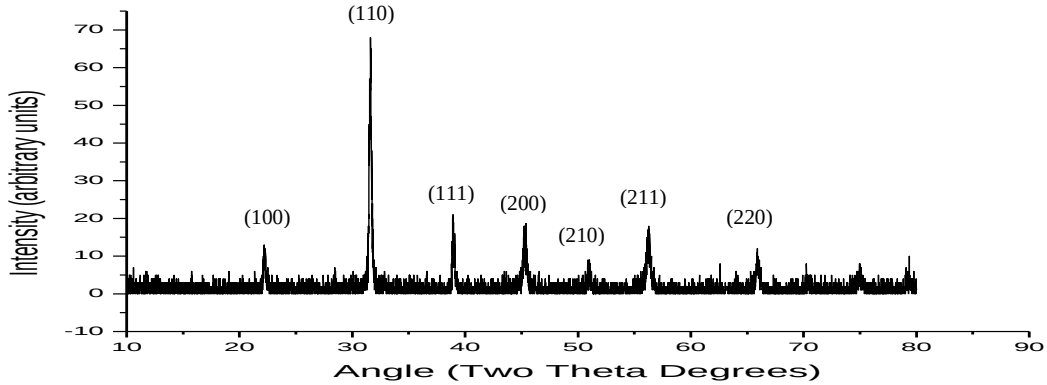

(c)

Fig. 3.4: XRD pattern of the samples sintered at 950^{o}C and milled for (a) 5 hrs (b) 10 hrs (c) 15 hrs.

3.3.1.1.2 SEM Analysis

Fig. 3.5 (a)-(c) shows the surface morphology of the samples milled for different duration using scanning electron microscope. A careful observation of the micrographs reveals porous and loosely packed grains for the samples milled for less duration. The samples prepared by milling for 15 hrs duration have very distinct boundaries and less porosity as compared to others. In case of the sample prepared after 10 hrs of milling duration, the porosity is quite high and the grains diffuse together in the region of contact. Also, it is observed that there is decrease in grain size with the increase in the milling duration.

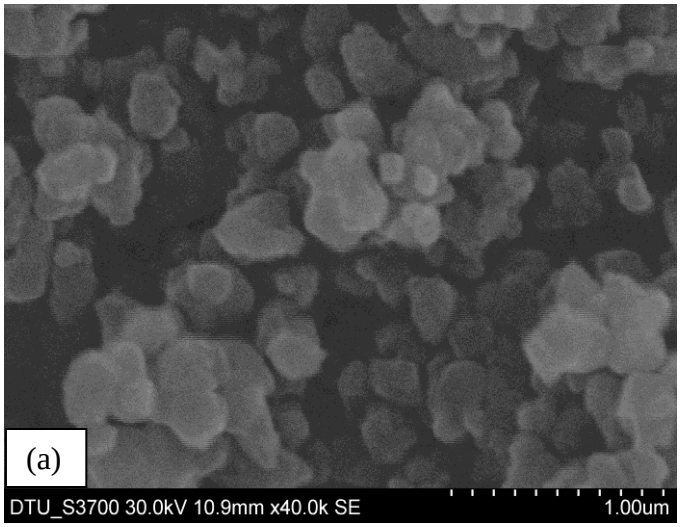

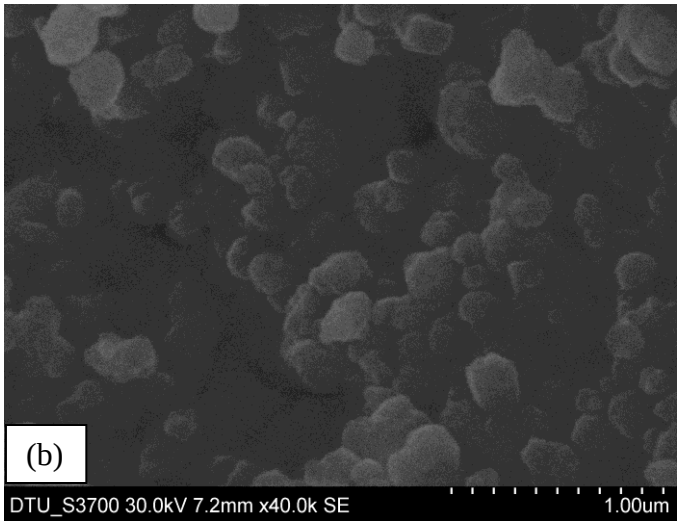

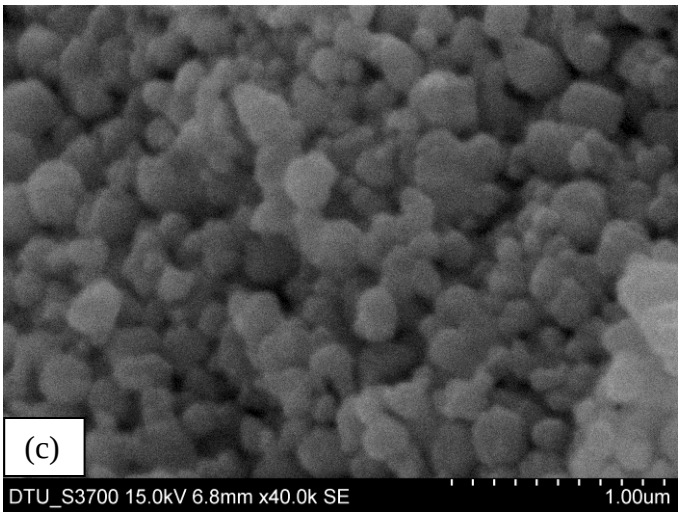

Fig. 3.5: SEM micrographs of the sample milled for: (a) 5 hrs, (b) 10 hrs, (c) 15 hrs.

3.3.1.2 Electrical Characterization

3.3.1.2.1 Dielectric studies

The dielectric properties i.e. dielectric constant (ϵ_r') and dielectric loss (tanδ) of the studied samples were measured. The variation of ϵ_r' and tanδ as a function of temperature at 10 kHz, 100 kHz and 500 kHz frequencies and the variation of ϵ_r' and tanδ with frequency at room temperature for different milling duration were measured and is presented below.

(A) Variation of ϵ_r' with temperature

Fig. 3.6(a)-(c) shows the temperature dependence of dielectric constant (ϵ_r') at the frequencies 10 kHz, 100 kHz and 500 kHz for the samples milled for different durations of 5 hrs, 10 hrs and 15 hrs respectively.

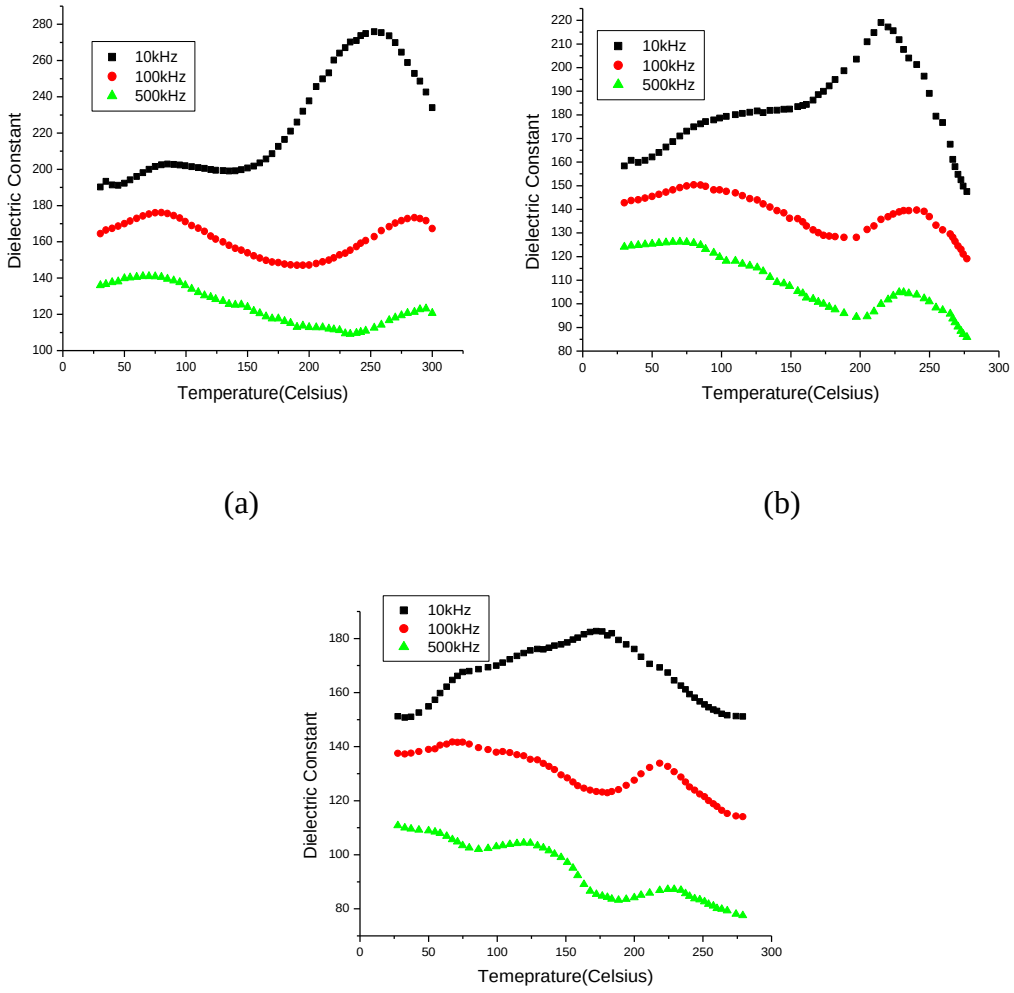

Fig. 3.6: Variation of dielectric constant with temperature of Iron substituted sample, $BaTi_{0.95}Fe_{0.05}O_3$ samples milled for: (a) 5 hrs, (b) 10 hrs and (c) 15 hrs at three different frequencies.

To see the effect of iron substitution in barium titanate on the ferroelectric to paraelectric phase transition temperature, the dielectric constant has been plotted with temperature at three different frequencies. The variation of dielectric constant with temperature for different milling durations i.e. 5 hrs, 10 hrs and 15hrs has been shown in Fig.3.6 (a), (b) and (c) respectively. The Barium Titanate shows the dielectric anomaly at a temperature called Curie Temperature (T_c) indicating the occurrence of ferroelectric-

paraelectric phase transition which is around 120^{o}C in the case of pure Barium Titanate as shown in Fig 3.2. The substitution of iron would tend to shift the Curie temperature to a lower temperature. A small kink has been observed at 70^{o}C approx as shown in Fig. 3.6 (a), (b) and (c), which might indicate the phase transition but not as sharply as is usually found in case of pure Barium Titanate. Also, the kink was not observed at the same temperature for all the frequencies which indicate the relaxor behavior.

To study the effect of milling duration on the value of dielectric constant, the curves have been plotted in Fig. 3.7(a), (b) and (c) at three different frequencies.

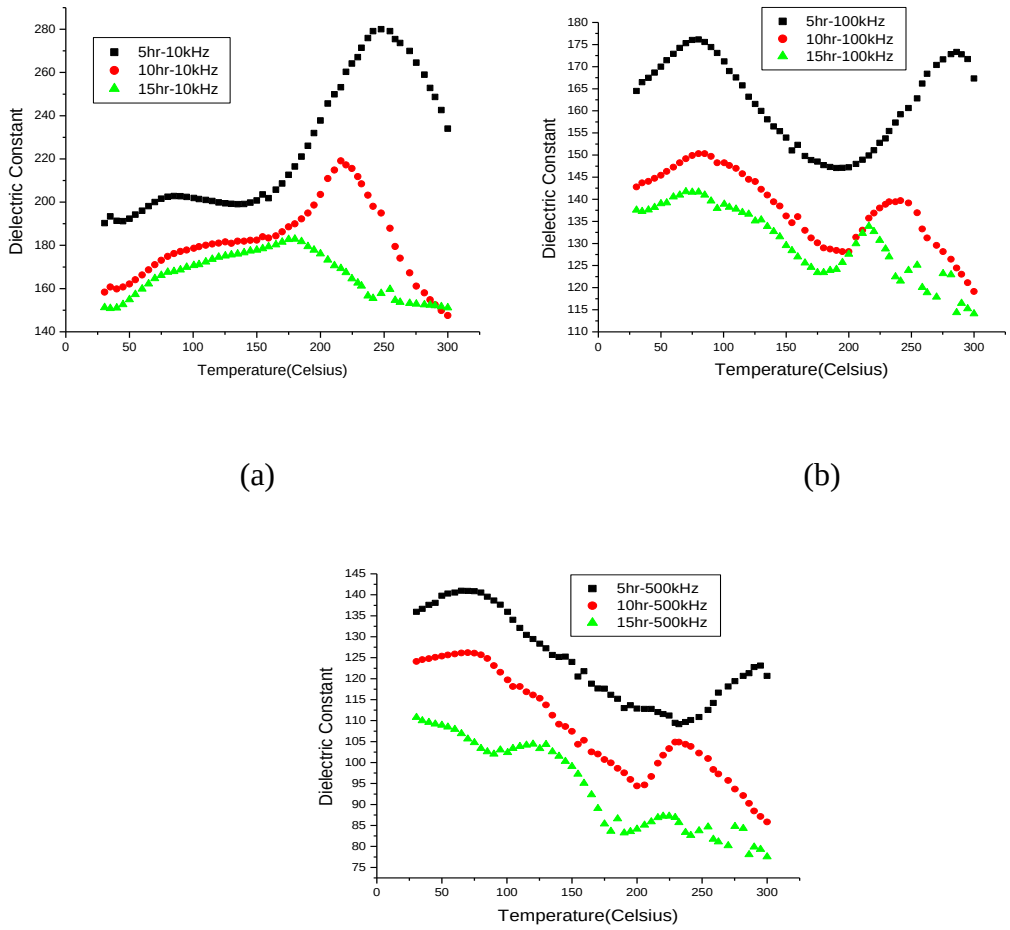

(a) (b)

(c)

Fig. 3.7: Variation of dielectric const. with temperature of $BaTo_{0.95}Fe_{0.05}O_3$ samples milled for different durations at three different frequencies of (a) 10kHz (b) 100kHz (c)500kHz.

The value of dielectric constant is highest for the 5 hrs milling duration and decreases as the milling duration is increased further. A reduction of dielectric constant with decreasing grain size occurs due to crystal distortion assisted by the surface atoms [1].

(B) Variation of dielectric loss (tanδ) with temperature

The dielectric loss for all the samples has been plotted. The dielectric loss should be as low as possible. Fig. 3.8(a)-(c) indicate the variation of dielectric loss with temperatures at three frequencies, 10 kHz, 100 kHz and 500 kHz for three different milling durations of 5 hrs, 10 hrs and 15 hrs respectively. The dielectric loss is almost constant initially but at higher temperatures it increases sharply. This sharp increase may be due to the increased mobility of space charges arising from defects [8].

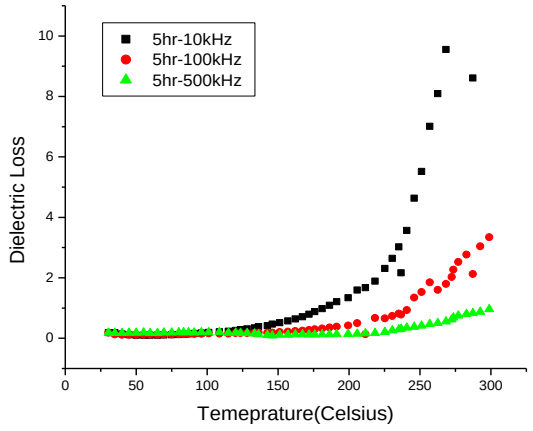

(a)

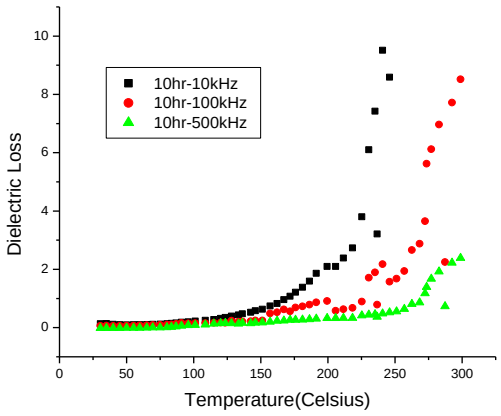

(b)

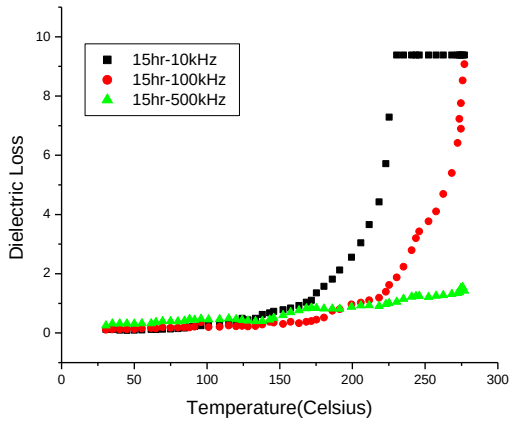

(c)

Fig. 3.8: Variation of dielectric loss with temperature at 1 kHz, 100 kHz and 500 kHz for three milling durations of (a) 5 hrs (b) 10 hrs (c) 15 hrs.

To see the effect of milling duration on the dielectric loss, the variations of dielectric loss with temperature for the milling durations of 5 hrs, 10 hrs and 15 hrs has been plotted in Fig.3.9 (a)-(c) at three different frequencies.

The dielectric loss is same for all the milling durations in lower temperature range and the increase at higher temperature takes place at different temperatures. The increase at higher temperature is less steep and occurs at higher temperature as the milling duration is increased. This may be attributed to the fact that the smaller particle size will cause less defects and hence less space-charge or interfacial polarization which causes less losses in the sample [9].

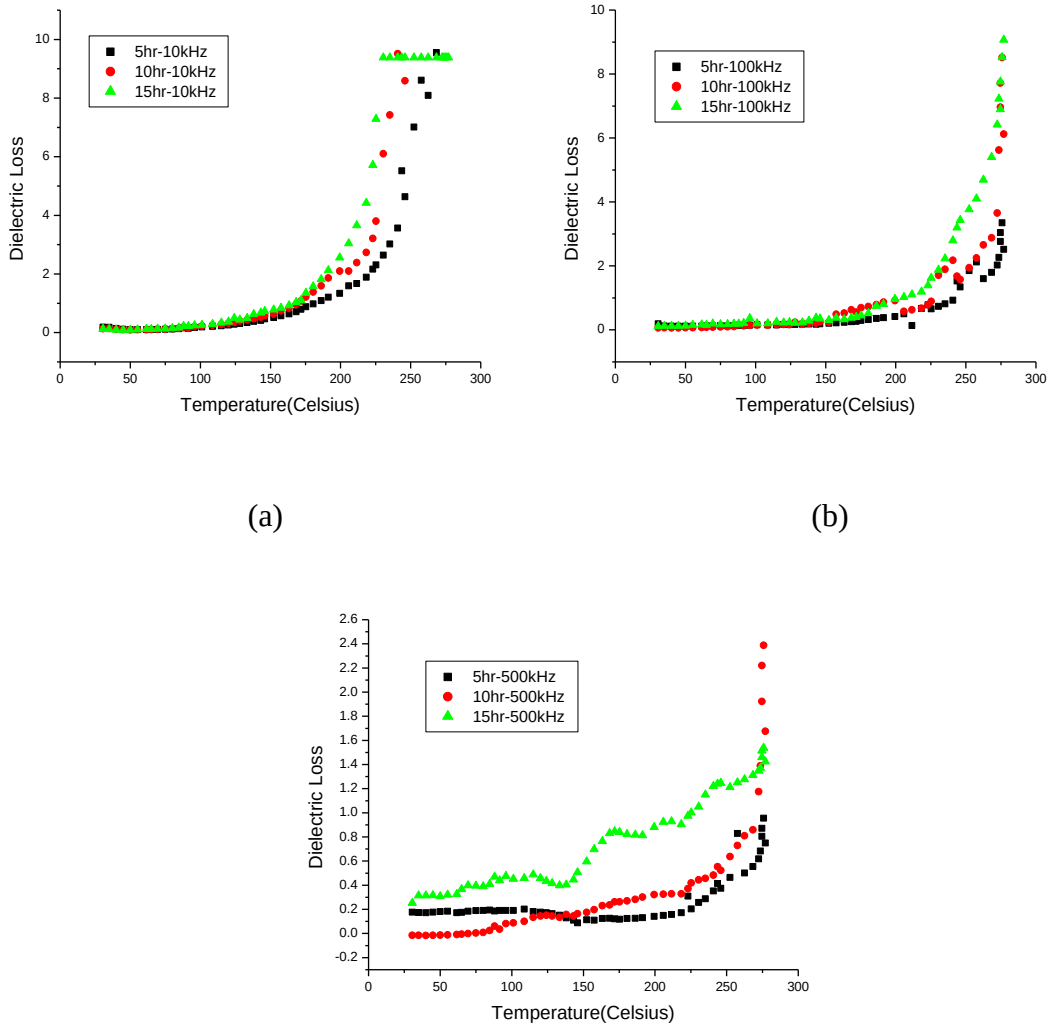

Fig.3.9: Variation of dielectric loss with temperature for milling durations of 5 hrs, 10 hrs and 15 hrs at frequencies: (a) 10 kHz (b) 100 kHz and (c) 500 kHz.

(C)Variation of ϵ_r' and tanδ *with frequency*

The variation of dielectric constant (ϵ_r') and dielectric loss (tanδ) as a function of frequency in the range of 20 Hz to 1 MHz at room temperature has been shown on fig. 3.10 (a) and (b) respectively.

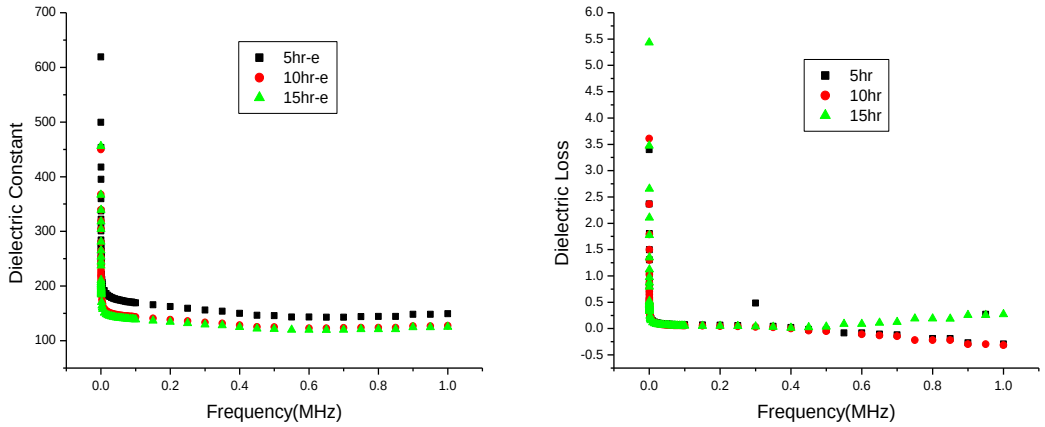

(a) (b)

Fig 3.10: Variation of dielectric constant and dielectric loss with wide frequency for three milling durations of 5 Hrs, 10 Hrs and 15 Hrs (a) dielectric constant with frequency, (b) dielectric loss with frequency.

As observed from the variation in Fig 3.10, the dielectric constant is high at lower side of the frequency range. As the frequency decreases, the dielectric constant becomes very high for almost all the milling durations. The higher values of dielectric constant at lower frequencies may be because of the presence of space charges in the structure which exist as defects. Moreover, at lower frequencies, the dipoles can follow the alternating electric field but at higher frequencies they may not be able to follow the alternations of the electric field leading to the reduction in the values of dielectric constant. The dielectric loss is almost same in all the cases but it also increases tremendously at lower frequencies which may be due to the same reasons [10].

3.3.1.2.2 Impedance analysis

Fig 3.11(a)-(c) shows the impedance (Z'-Z") plots at some selected temperatures of the studied specimens.

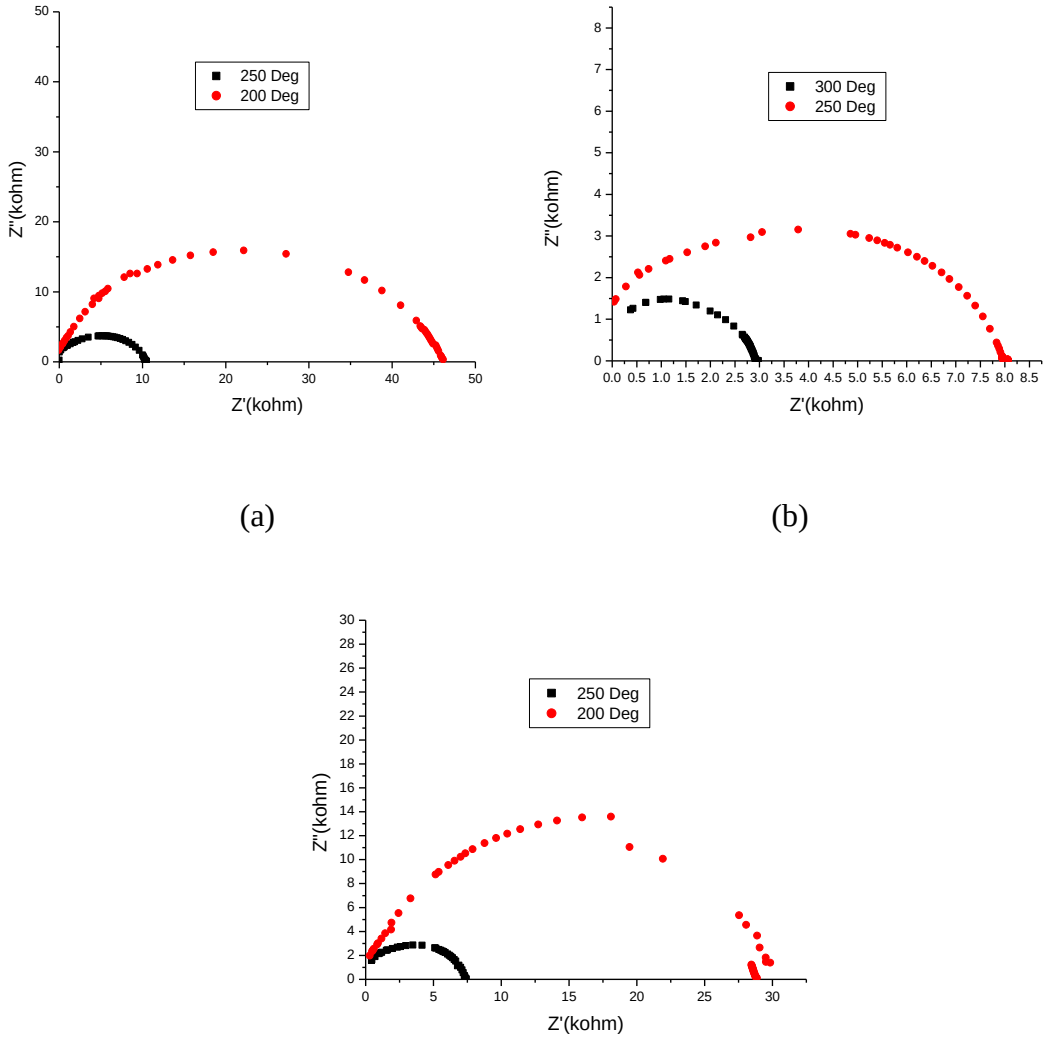

Fig. 3.11: Complex impedance spectrum (Cole-Cole plots) of $BaTi_{0.95}Fe_{0.05}O_3$ at different temperatures for the milling duration of: (a) 5 hrs (b) 10 hrs and (c) 15 hrs respectively.

All the semicircles in the Cole-Cole plots exhibit some depression instead of a proper semicircle arc around the x-axis. This indicates that there is a distribution of relaxation time instead of a single relaxation time in the material [12].

It can be noted that the plot obtained for the milling duration of 15 hours has two

semi-circles at higher temperature (250^{o}C). This implies the presence of both bulk property and grain boundary effects for this particular milling duration. This may be because as the size reduces the grain boundaries increases and hence the contribution of grain boundaries observed. The value of bulk resistance (R_b) at different temperatures for different milling durations have been obtained from the intercept of the semi-circular arcs on the real axis (Z') and are given in Table 3.1.

It has been observed that R_b decreases with rise in the temperature for all the samples. With respect to milling duration, of all the values, the value of R_b for 10 hrs milling duration is lowest.

Table 3.1 Bulk resistance obtained from Cole-cole graph

Measuring Temperature / **Milling Duration**	**250^{o}C** R_b	**200^{o}C** R_b
5 hours	**10.271kΩ**	**46.265kΩ**
10 hours	**2.937kΩ**	**7.980kΩ**
15 hours	**7.289kΩ**	**28.905kΩ**

3.3.1.2.3 Ferroelectric studies

Fig. 3.12 shows the room temperature P-E hysteresis loops of $BaTi_{0.95}Fe_{0.05}O_3$ compound prepared by milling the sample for different durations. The corresponding values of remanent polarization ($2P_r$) and coercive field ($2E_c$) are tabulated in Table 3.2.

It is known that the P-E hysteresis loops are microstructure dependent [13]. A densely packed microstructure with uniformly distributed grains and sharp and distinct grain boundaries in the sample results in the formation of the hysteresis loop. This is the case as seen in Fig. 3.10 for 5 hrs milling duration. For 15 hrs milled sample, a lossy kind of hysteresis loop is obtained which could be related to higher dielectric loss in the sample.

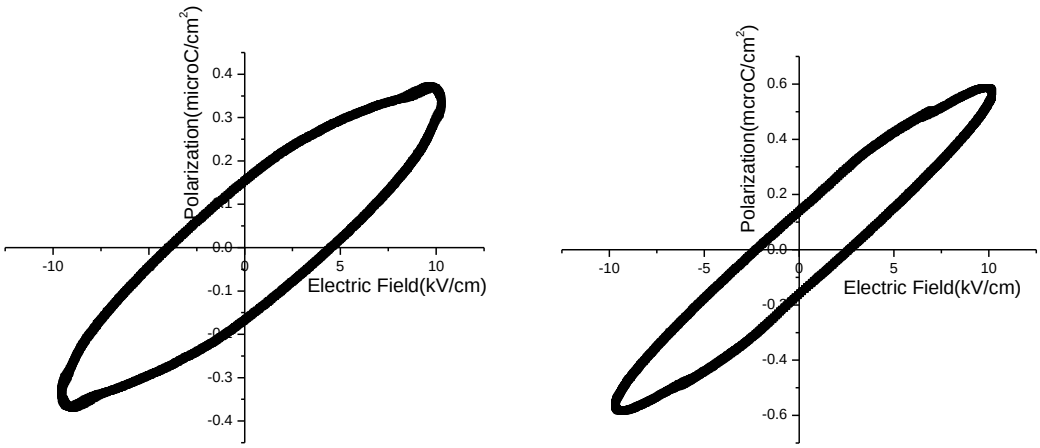

(a) (b)

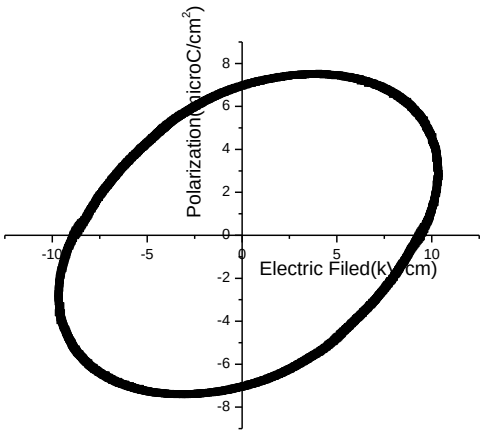

(c)

Fig. 3.12: P-E hysteresis loops of the studied samples milled for (a) 5 hrs (b) 10 hrs and (c) 15 hrs

The table 3.2 shows that the remanent polarization for the sample milled for 5 hrs is more than that of the sample milled for 10hrs. But the remanent polarization is maximum in the case of 15 hrs milling duration.

Table 3.2: $2P_r$ and $2E_c$ of the samples milled for different durations.

Milling Duration	$2P_r$ ($\mu C/cm^2$)	$2E_c$ (kV/cm)
5 hour	0.15	10.26
10 hour	0.14	10.17
15 hour	6.93	10.13

3.3.2 Optimization of sintering Temperature

The $BaTi_{0.95}Fe_{0.05}O_3$ samples have been sintered at two different temperatures in order to study the effect of sintering temperature. The earlier discussed results were of the same sample but milled for different durations. But, here we present a discussion of the samples sintered at two temperatures i.e. 950^oC and 1150^oC. The electrical characterization has been studied here in detail.

3.3.2.1 Electrical Characterization

3.3.2.1.1 Dielectric Studies

The dielectric properties i.e. dielectric constant (ϵ_r') and dielectric loss (tanδ) of the studied samples were measured. The variation of ϵ_r' and tanδ at three different frequencies and the variation of ϵ_r' and tanδ with frequency at room temperature for different sintering conditions were measured and is presented here.

(A) Variation of ϵ_r' with temperature: Curie temperature

Fig. 3.13 shows the variation of dielectric constant (ϵ_r') with temperature for the samples sintered at 950^oC and 1150^oC for three different frequencies of 10 kHz, 100 kHz and 500 kHz.

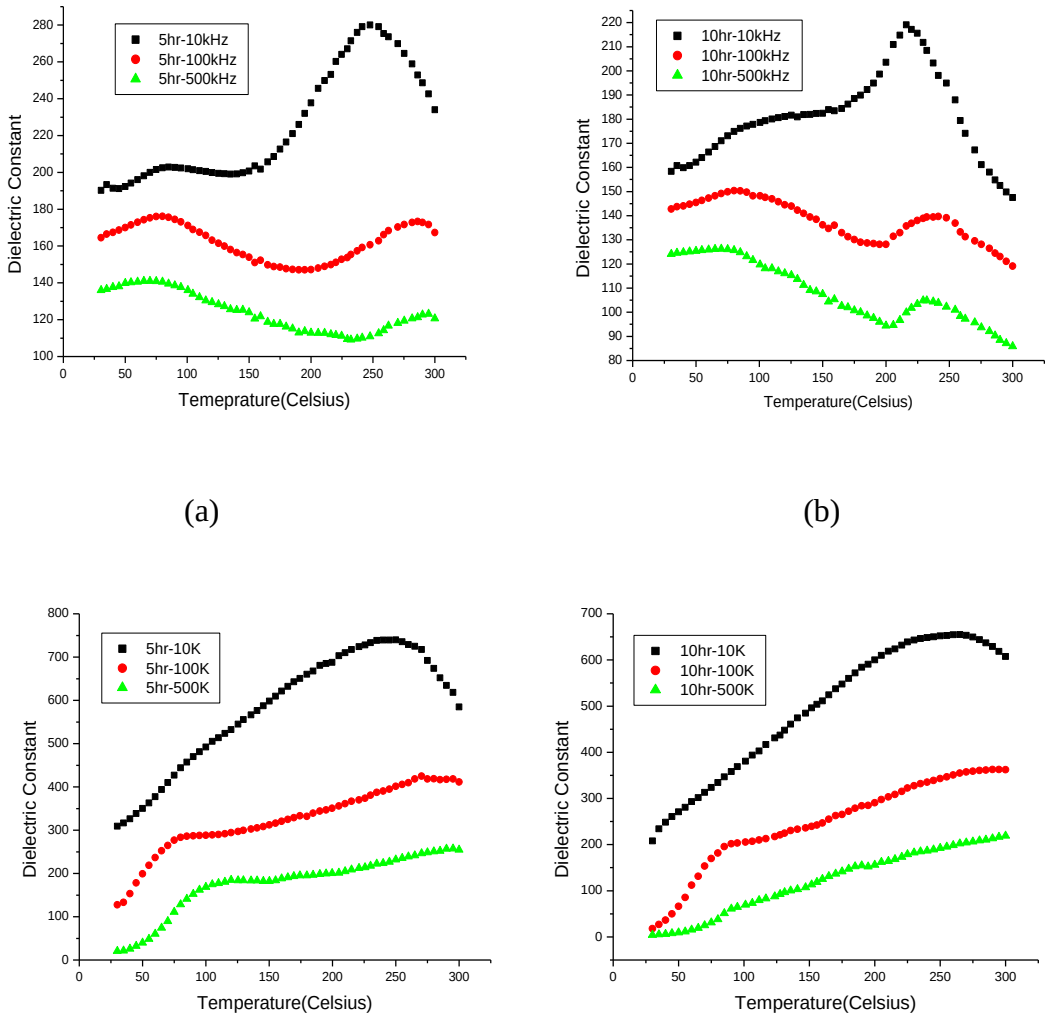

Fig. 3.13: Variation of dielectric constant with temperature at two sintering temperatures of (a) 950^{o}C, 5hrs milling (b) 950^{o}C, 10hrs milling (c) 1150^{o}C, 5hrs milling (d) 1150^{o}C, 10 hrs miiling.

The behavior of dielectric with temperature change has been shown above. For both the sintering conditions, the compound show dielectric phase transition at a temperature called Curie temperature. Although a very sharp phase transition has not been observed in iron substituted Barium Titanate, a small kink is present near 70^{o}C. But this kink is present at slightly different temperatures at different frequencies in all the samples sintered at

same temperature and same milling duration. This indicates the relaxor behavior of iron substituted Barium Titanate. The kink near T_c shows a suppressed ferroelectric behavior. Now, in order to see the effect of sintering temperature, plot the graph at each frequency for the two sintering conditions

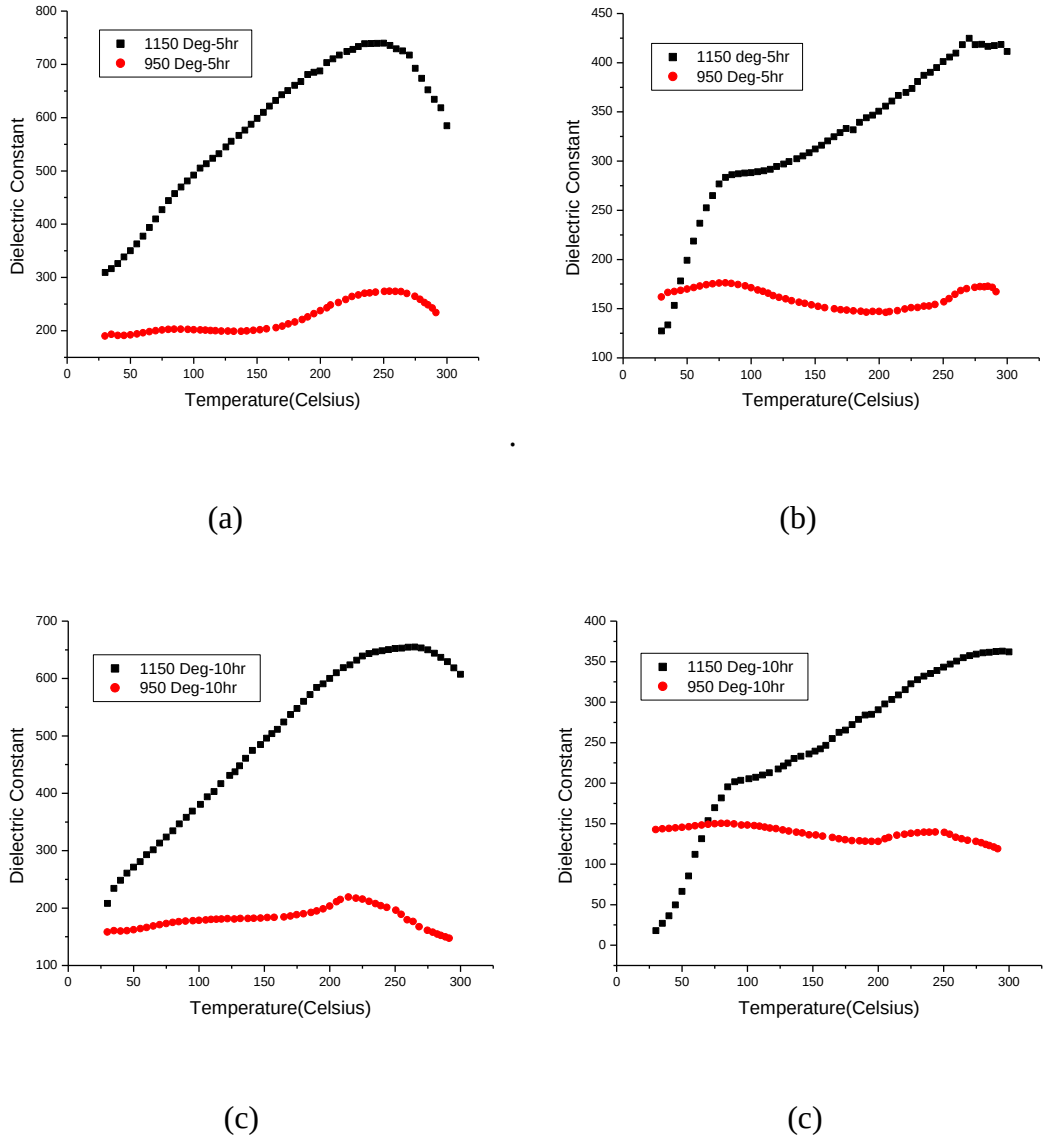

Fig. 3.14: Variation of dielectric constant for different sintering temperature at (a) 5 hrs milling, 10 kHz (b) 5 hrs milling, 100kHz (c) 10 hrs milling, 10kHz (d) 10hrs milling, 100 kHz.

It has been observed from Fig. 3.14 that the value of dielectric constant increases

with the increase in sintering temperature. The increase in ϵ_r' can be understood by the increase in the grain size with increase in sintering temperature. The higher sintering temperature increases the average grain size, making the domain wall motion easier resulting in an increased polarization and subsequently increasing the dielectric constant [14].

(B) Variation of dielectric loss (tanδ) with temperature

In order to see the effect of sintering temperature on the variation of dielectric loss with temperature, the curves have been plotted in Fig. 3.15(a)-(f) at three different frequencies for milling durations of 5 hrs and 10 hrs.

As observed from the Fig. 3.15, the dielectric loss is more at lower temperatures for higher sintering temperature for 5 hrs milling duration but at higher temperature, it is lower for the sample with lower sintering temperature. The loss for 10 hrs milling duration is low at higher sintering temperature.

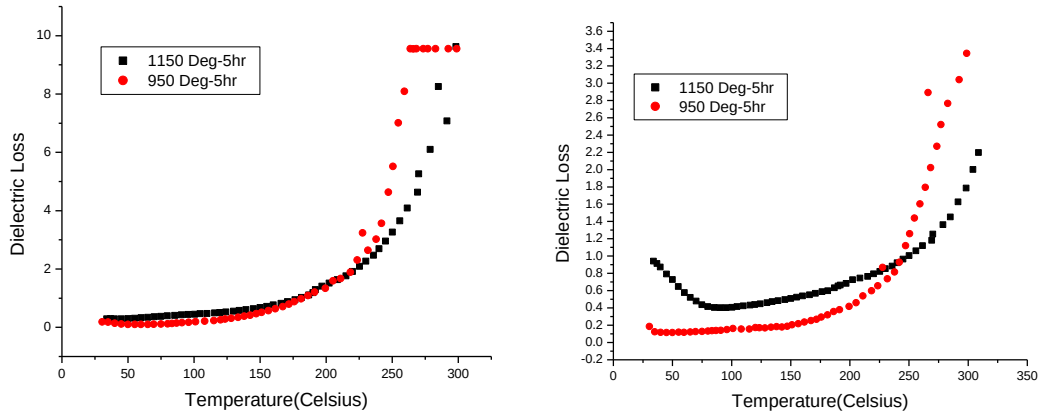

(a) (b)

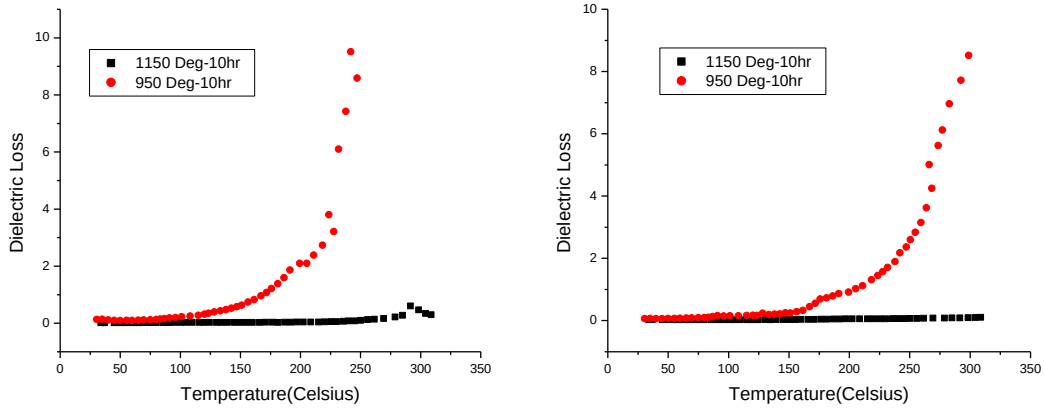

(c) (d)

Fig. 3.15: Variation of dielectric loss with temperature for sintering temperature of 950^{o}C and 1150^{o}C at (a) 5 hrs milling, 10 kHz (b) 5 hrs milling, 100kHz (c) 10 hrs milling, 10kHz (d) 10hrs milling, 100 kHz.

(C) Variation of ϵ_r' and **tanδ** *with frequency*

Fig. 3.16 shows the variation of dielectric constant (ϵ_r') and dielectric loss (tanδ) with frequency.

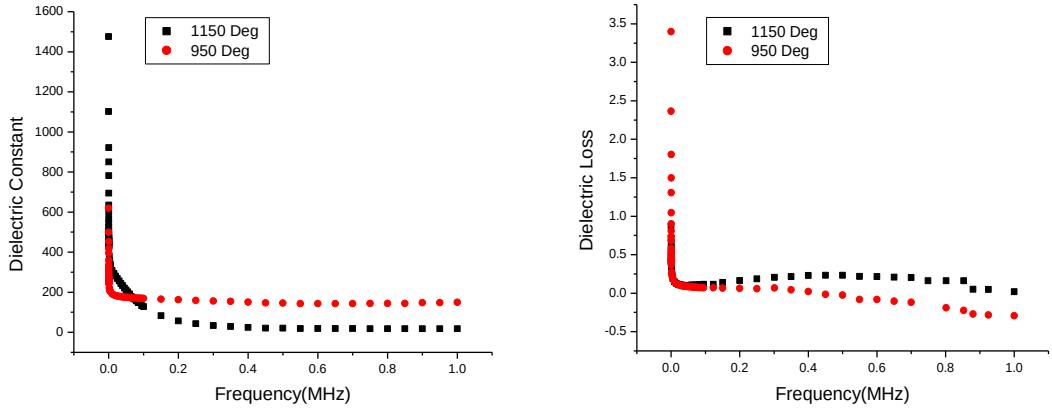

(a) (b)

Fig. 3.16: Variation with frequency at sintering temperature of 1150^{o}C and 950^{o}C for 5 hrs milling duration of (a) Dielectric Constant (b) Dielectric Loss.

The behavior with frequency for both the sintering temperature of 1150^{o}C and 950^{o}C of dielectric constant and dielectric loss is same.

3.3.2.1.2 Impedance Analysis

The impedance plots (Z'-Z") plots for different sintering temperature of studied samples are shown in Fig. 3.17. All the Cole-Cole plots exhibit some depression instead of a semi-circle centered on the x-axis. This shows that samples prepared under given set of conditions exhibit the relaxor behavior.

It can be noted that in the samples sintered at higher temperature exhibit two semicircles for the samples milled for 5 hrs and 10 hrs. This implies the presence of both grain and grain boundary effects for this sintering condition. Though in section 3.2.2.2 the same effect has been observed for the sample milled for 15 hrs. Both can be justified as: In this case, at higher sintering temperature, grain boundaries develop properly causing the grain boundary effect to be effective and in the previous case, the increased milling duration reduces the particle size, thereby, increasing the grain boundaries and hence the grain boundary effect.

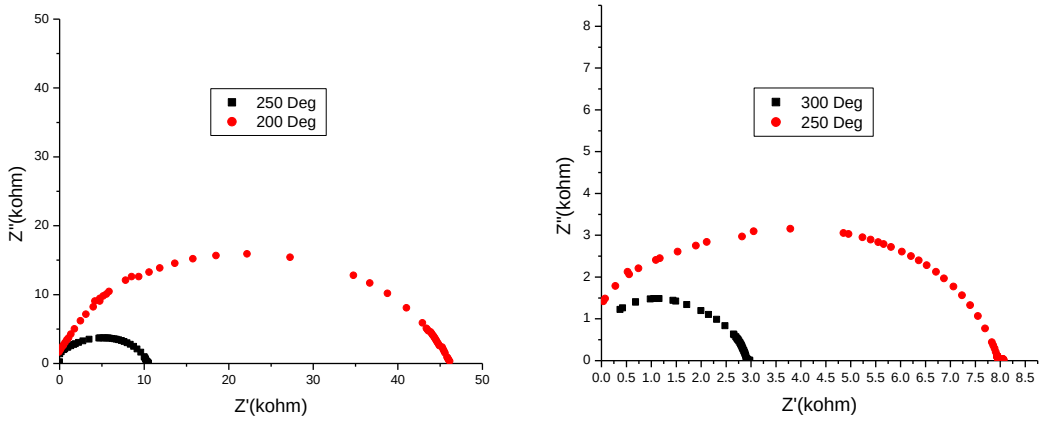

(a) (b)

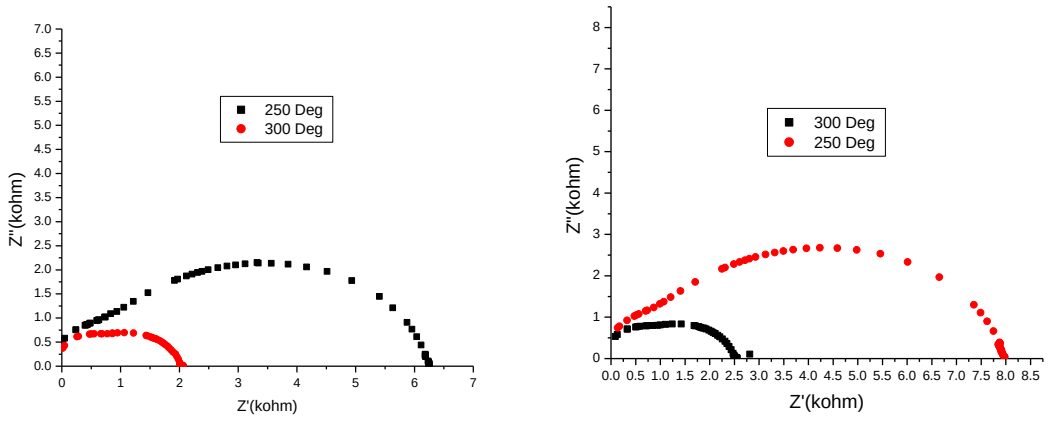

(c) (d)

Fig. 3.17: Complex impedance spectrum (Cole-Cole) of BaTi0.95Fe0.05O3 sample at (a) 950oC, 5 hrs milling (b) 950oC, 10 hrs milling (c) 1150oC, 5 hrs milling (d) 1150oC, 10 hrs milling.

3.3.2.1.3 Ferroelectric studies

The effect of sintering temperature on the ferroelectric property has been studied of the prepared samples. The P-E hysteresis loops for sintering temperature of 950^{0}C and 1150^{o}C are shown in Fig.3.18.

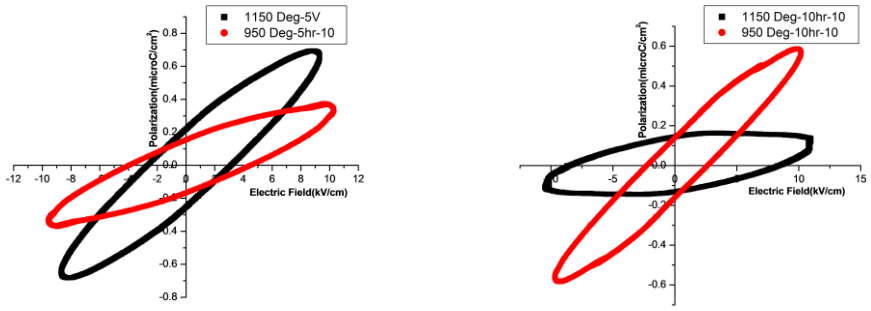

(a) (b)

Fig. 3.18: P-E hysteresis loops for sintering temperature of 950^{o}C and 1150^{o}C for (a) 5 hrs milling (b) 10 hrs milling.

From the hysteresis loop obtained for different sintering temperature, it has been observed that the remanent polarization of the samples sintered at 950^{o}C and 1150^{o}C is almost same for both the milling durations.

References

[1] A. Jana, T. K. Kundu, S. K. Pradhan and D. Chaksavorty, J. of App. Phys. **97** (2005)

044311.

[2] J. W. Kim, J. G. Heinrich, J. Eur. Ceram. Soc. **25** (2005) 1637.

[3] H. Kungla and M. J. Hoffman, J. Appl. Phys. 107 (2010) 054111-1.

[4] A. Yang, C. A. Wang, R. Guo, Y. Huang, C. W. Nan, Ceram. Int. **36 (**2010) 549.

[5] B. Su, J. E. Holmes, B. L. Cheng and T. W. Button, J. Electroceram. 9 (2002).

[6] X. Deng, X. Guan, P. Chen, C. Lu, Z. Tan, D. Li, J. Li, X. Wang and L. Li, Thin Solid

Films 518 (2010) e75-e77.

[7] S. Jayanthi, T. R. N. Kutty, J. Mater. Sci: Mater Electron (2008) 19:615-626.

[8] T. Freissnegg, S. Aggarwal, R. Ramesh, B. Nielsen, E. H. Poindexter and D. J. Keeble,

Appl. Phys. Lett. 77 (2000) 127.

[9] A. Chen, Y. Zhi and L. E. Cross, Phys. Rev. B **62** (2000) 228.

[10] W. L. Warren, K. Vanheusden, D. Dimos, G. E. Pike and B. A. Tuttle, J. Am.

Ceram. Soc. 78 (1995) 536.

[11] M. M. Vijatović, J. D. Bobić, B. D. Stojanović, Scieno of Sintering, **40** (2008) 155-165.

[12] S. Sen, R. N. P. Choudhary and P. Pramanik, Phys. B **387** (2007) 56.

[13] G. Li, L. Zheng, Q. Yin, B. Jiang and W. Cao, J. Appl. Phys. **98** (2005) 064108-1.

Chapter 4

Conclusion & Future scope

4.1 Conclusion

In this chapter, a recapitulation of the main results obtained in the present work has been summarized and inferences have been drawn. Also, the scope for the future work has been put forth.

In the present work, a study of the structural and electrical characterization has been studied to see the changes in the properties after a substitution at B-site. Moreover, the optimized milling duration has been found. The properties change at different sintering temperature has been studied too.

The samples studied in the present work were prepared through mechanical activation method. This method reduces the need of high energy consuming calcinations step. It has been observed that the sample phase has been obtained by sintering the sample at lower temperature (in this case $950^{o}C$) as compared to other methodologies which require higher temperature of about $1200^{o}C$ or more.

Firstly, the milling duration has been optimized to synthesize $BaTi_{0.95}Fe_{0.05}O_3$ compound. It was found that the optimized milling duration to prepare $BaTi_{0.95}Fe_{0.05}O_3$ is 5 hours. For 5 hours of milling duration, we obtain the highest dielectric and lowest dielectric loss out of three. The remanent polarization ($2P_r$) for this sample is found to be $0.15\mu C/cm^2$.

Also, the substitution at B-site has shown a change in the ferroelectric to paraelectric phase transition condition. In Barium Titanate, usually, the ferroelectric to paraelectric phase transition takes place at $130^{o}C$. But the substitution at the B-site shifts the transition

temperature to a lower value (around 70^{o}C approx.). Moreover, the transition from ferroelectric to paraelectric phase is not very sharp but a small kink has been observed. This implies that the ferroelectric character has been suppressed.

For the seeing the effect of sintering temperature, the samples of same composition has been prepared by sintering them at a higher temperature of 1150^{o}C. The effect of sintering temperature has been studied by electrical characterization.

It has been found that the samples prepared by sintering at higher temperature of 1150^{o}C have a higher dielectric constant than the samples prepared by sintering at a temperature of 950^{o}C. Moreover, the dielectric loss is lesser in case of samples sintered at 1150^{o}C. Hence, as the sintering temperature is increased, both the above said characteristics improve. From the Cole-cole plot, it has been found that the samples sintered at higher sintering temperature exhibit the contribution of grain and grain boundaries (concluded from the two semi-circles in Cole-cole plot). The ferroelectric property shows that the remanent polarization is almost same for the samples sintered at different temperatures.

4.2 Future Prospects

In the present work, Barium Titanate has been studied by substitution of Iron (Fe) at the titanium site i.e. B-site. The results obtained show a change in the characteristics. But in the pervoskite structured Barium Titanate, the substitution can be done at both A-site and B-site. The B-site substitution has been done and characterized.

The substitution at A-site can be taken up to understand the influence of substitution on the properties of the sample and hence can be compared with the results obtained by substitution at B-site. This would help further to get an element with better dielectric properties which could be used for commercial purpose.